universidade de aveiro
Departamento de Eletrónica, Telecomunicações e Informática

Francisco João Melim Machado de Oliveira

Pré-codificação e Equalização para Sistemas SC-FDMA Heterogéneos

Precoding and Equalization Schemes for SC-FDMA Heterogeneous Networks

universidade de aveiro Departamento de Eletrónica, Telecomunicações e Informática

Francisco João Melim Machado de Oliveira

Pré-codificação e Equalização para Sistemas SC-FDMA Heterogéneos

Precoding and Equalization Schemes for SC-FDMA Heterogeneous Networks

Dissertação apresentada à Universidade de Aveiro para cumprimento dos requisitos necessários à obtenção do grau de Mestre em Engenharia Eletrónica e Telecomunicações, realizada sob a orientação científica do Doutor Adão Silva (orientador), Professor Auxiliar e do Doutor Atílio Gameiro (coorientador), Professor Associado, ambos do Departamento de Eletrónica, Telecomunicações e Informática e do Instituto de Telecomunicações - Aveiro.

Dedico este trabalho aos meus pais Adolfo Jorge e Maria de Lurdes e aos meus colegas, amigos, professores e familiares que me apoiaram e ajudaram ao longo deste percurso.

o júri / the jury

presidente / president	Prof. Doutor José Rodrigues Ferreira da Rocha Professor Catedrático da Universidade de Aveiro
vogais / examiners committee	Prof. Doutor Carlos Miguel Nogueira Gaspar Ribeiro Professor Adjunto do Instituto Politécnico de Leiria
	Prof. Doutor Adão Paulo Soares da Silva Professor Auxiliar da Universidade de Aveiro (Orientador)

agradecimentos

Agradeço aos meus orientadores Doutor Adão Silva e Doutor Atílio Gameiro por mostrarem-se sempre disponíveis para ajudar com qualquer dúvida ou problema relativo ao meu trabalho.

Aos meus colegas no ramo das comunicações móveis agradeço a ajuda e companheirismo durante o tempo passado no Instituto de Telecomunicações.

À Universidade de Aveiro, aos professores e alunos do Departamento de Eletrónica e Telecomunicações tenho a agradecer o apoio demonstrado nos anos que cá estive.

Por fim agradeço aos meus pais, irmão, familiares e amigos por toda a ajuda e apoio demonstrado ao longo da minha vida.

palavras-chave OFDMA, SC-FDMA, IB-DFE, IA, Heterogeneous Network.

resumo

O trafego móvel nas redes celulares tem aumentado exponencialmente. As pico-células são consideradas como a solução chave para cumprir estes requisitos. Dentro do mesmo espectro, as pico-células e as macro-células (formando os chamados sistemas heterogéneos) precisam de colaborar de modo a que um sistema possa adaptar-se ao outro. Se não for considerada a cooperação, então as pico-células irão gerar interferência prejudicial na macro-célula.

Interference alignment (IA) é uma técnica de précodificação que é capaz de atingir o grau máximo de liberdade do canal de interferência, e consegue lidar eficazmente com interferência entre sistemas. Single carrier frequency division multiple access (SC-FDMA) é uma solução técnica promissora para transmissão de dados em uplink, para sistemas celulares futuros. Equalizadores lineares convencionais não são eficientes a remover a interferência residual entre portadoras dos sistemas SC-FDMA. Por este motivo, tem havido interesse significativo no desenho de equalizadores não lineares no domínio da frequência em geral e em equalizadores baseados em decisão por feedback em particular, tendo o iterative block decision feedback equalizer (IB-DFE) como o equalizador não linear mais promissor.

Nesta dissertação propomos e avaliamos précodificação de alinhamento de interferência nos terminais das pico-células em conjunto com equalizadores não lineares no domínio da frequência nos recetores (estação base da macro-célula e unidade central de processamento) para redes heterogéneas baseadas em SC-FDMA. Os précodificadores das pico-células são desenhados de maneira a obrigar a que toda a interferência gerada na macro-célula esteja alinhada num subespaço ortogonal em relação ao subespaço do sinal recebido na macro-célula. Isto obriga a que não seja observada degradação de desempenho na macro-célula. Em seguida, desenhamos um equalizador não linear no domínio da frequência no recetor da macro-célula capaz de recuperar os fluxos de dados da macro-célula, na presença de interferência tanto entre portadoras como das pico-células. Os resultados mostram que as estruturas de transmissão e receção propostas são robustas contra a interferência entre sistemas e ao mesmo tempo capaz de separar eficientemente os dados da macro e das pico células.

keywords OFDMA, SC-FDMA, IB-DFE, IA, Heterogeneous Network.

abstract

Mobile traffic in cellular networks is increasing exponentially. Small-cells are considered as a key solution to meet these requirements. Under the same spectrum the small-cells and the associated macro-cell (forming the so called heterogeneous systems) must cooperate so that one system can adapt to the other. If no cooperation is considered then the small-cells will generate harmful interference at the macro-cell.

Interference alignment (IA) is a precoding technique that is able to achieve the maximum degrees of freedom of the interference channel, and can efficiently deal with inter-systems interference. Single carrier frequency division multiple access (SC-FDMA) is a promising solution technique for high data rate uplink communications in future cellular systems. Conventional linear equalizers are not efficient to remove the residual inter-carrier interference of the SC-FDMA systems. For this reason, there has been significant interest in the design of nonlinear frequency domain equalizers in general and decision feedback equalizers in particular, with the iterative block decision feedback equalizer (IB-DFE) being the most promising nonlinear equalizer.

In this dissertation we propose and evaluate joint interference alignment precoding at the small cell user terminals with iterative non-linear frequency domain equalizer at the receivers (macro base station and central unit) for SC-FDMA based heterogeneous networks. The small-cell precoders are designed by enforcing that all generated interference at the macro-cell is aligned in an orthogonal subspace to the macro-cell received signal subspace. This enforces that no performance degradation is observed at the macro cell. Then, we design an iterative nonlinear frequency domain equalizer at the macro-cell receiver that is able to recover the macro-cell spatial streams, in the presence of both small-cell and inter-carrier interferences. The results show that the proposed transmitter and receiver structures are robust to the inter-system interferences and at the same time are able to efficient separate the macro and small cells spatial streams.

Table of Contents

List of Figures

List of Acronyms

BS	Base Station
UT	User Terminal
CPU	Central Pressing Unit
MIMO	Multiple-Input and Multiple-Output
ISI	Inter-Symbol Interference
SC	Single Carrier
MC	Multi-Carrier
OFDM	Orthogonal Frequency-Division Multiplexing
FDE	Frequency-Domain Equalization
DFT	Discrete Fourier Transform
FFT	Fast Fourier Transform
IFFT	Inverse Fast Fourier Transform
DFE	Decision Feedback Equalization
CP	Cyclic Prefix
IB-DFE	Iterative-Block Decision Feedback Equalization
BER	Bit Error Rate
MFB	Matched Filter Bound
OFDMA	Orthogonal Frequency Division Multiple Access
SC-FDMA	Single-Carrier with Frequency Division Multiple Access
QPSK	Quaternary Phase Shift Keying
SNR	Signal-to-Noise Ratio
NSR	Noise-to-Signal Ratio
SQNR	Signal-to-Quantization-Noise Ratio
MSE	Mean Square Error
MMSE	Minimum Mean Square Error
ADC	Analog-to-Digital Converter
DAC	Digital-to-Analog Converter

PDP	Power Delay Profile
PSD	Power Spectrum Density
SINR	Signal to Interference-plus-Noise Ratio
ZF	Zero-Forcing
PMEPR	Peak-to-Mean Envelope Power Ratio
MUD	Multiuser Detection
FDM	Frequency Division Multiplexing
PSD	Power Spectrum Density
LLR	LogLikelihood Ratio
SIC	Successive Interference Cancelation
PCM	Pulse Code Modulation
SDR	Signal-to-Distortion Ratio
IA I	Interference Alignment
HetNet	Heterogeneous Network
PAPR	Peak to Average Power Ratio

1. Introduction

1.1 Context

1.1.1 Arriving at the LTE

Work towards a new standard called Long Term Evolution (LTE) defined by 3GPP (3rd Generation Partnership Project) started in 2004 by defining targets. Since it takes more than 5 years from starting a project until commercial deployment, it is necessary to start defining standards early enough that when the need arises, it is ready to deploy. The need for LTE is the same as with all communications technology: wireline capability evolution, more wireless capacity and lower cost in data delivery. Wireline technology keeps evolving and so must the wireless domain to keep up with demand. Competition also is a driving factor since 3GPP isn't the only entity developing new wireless technologies. More capacity is a major requisite for taking advantage of the available spectrum and base stations [1].

LTE was designed to deliver higher performance when compared to existing technologies based on HSPA (High Speed Packet Access) technology. The performance targets were defined in 3GPP

release 6. The peak throughput should be 100 Mbps in downlink and 50 Mbps in uplink, ten times higher than HSPA release 6. The latency, a major problem should also be largely reduced as well as lower terminal power consumption to enable more multimedia applications with a single battery charge. The main performance targets are:

- Spectral efficiency 2-4 times more than HSPA release 6.
- Peak rates of 100 Mbps in downlink and 50 Mbps in Uplink.
- Latency below 10 ms.
- Optimized for packet switching.
- High level of mobility and security.
- Optimized power efficiency.
- Frequency flexibility from 1.5 MHz to 20 MHz [1].

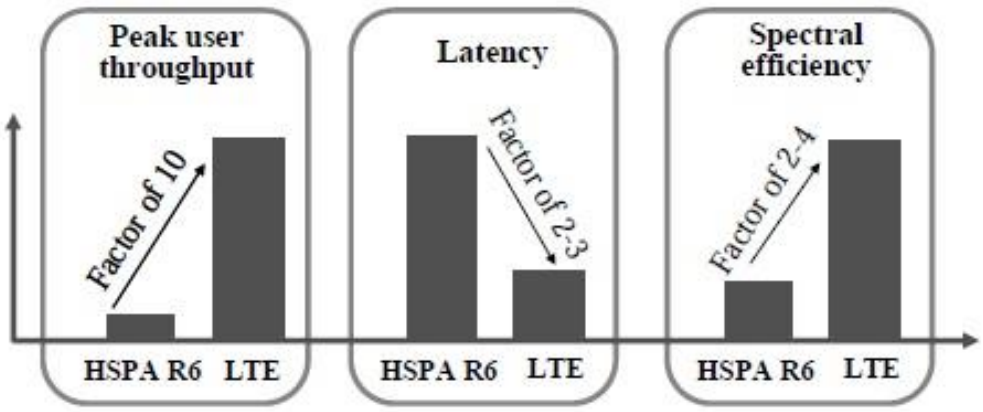

Figure 1.1 Main LTE performance targets

LTE uses for downlink a multiple access scheme known as Orthogonal Frequency Division Multiple Access (OFDMA) and Single Carrier Frequency Division Multiple Access (SC-FDMA) for the uplink. These solutions provide orthogonality between the users, greatly reducing the interference and improving the overall capacity of the network. In the frequency domain, the resource allocation is done with blocks of 180 KHz both for uplink and downlink. The high LTE capacity comes from this frequency dimension in the packet scheduling. For the uplink the user specific allocation is continuous, while for the downlink resource blocks can be used from any part of the available spectrum. The solution used for the uplink is designed to allow for more efficient power amplifier design, which translates directly into the terminal battery life. The solution used in LTE allows spectrum flexibility since the transmission bandwidth can be selected between 1.4 MHz and 20 MHz depending on the available spectrum. The maximum of 20 MHz bandwidth combined 2x2 MIMO can provide peak 150 Mbps downlink user data rate, increasing to 300 Mbps with 4x4 MIMO. The uplink peak data rate stays at 75Mbps [1].

The multiple access schemes used in LTE are shown in figure 1.2

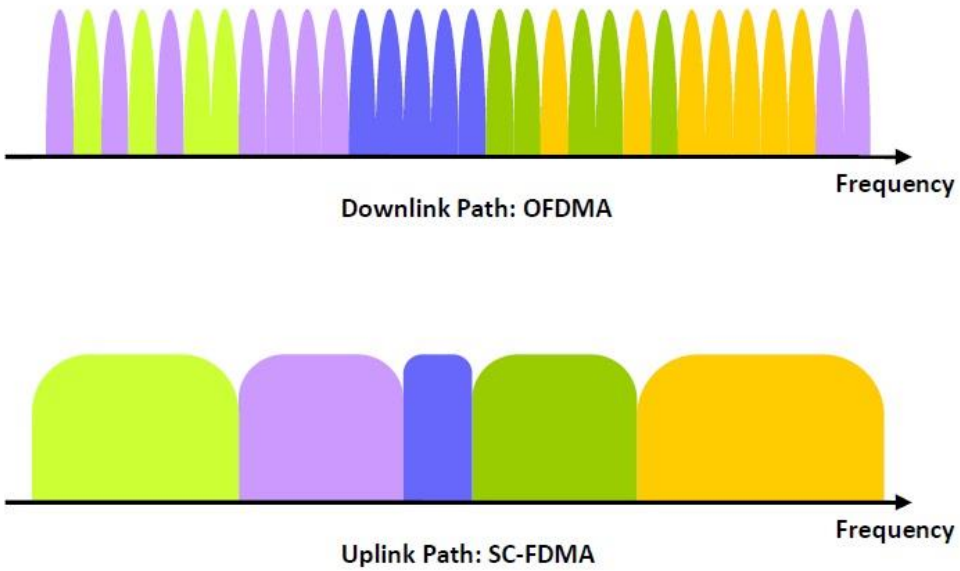

Figure 1.2 LTE multiple access schemes

The higher network capacity also needs a more efficient network architecture, as shown in figure 1.3

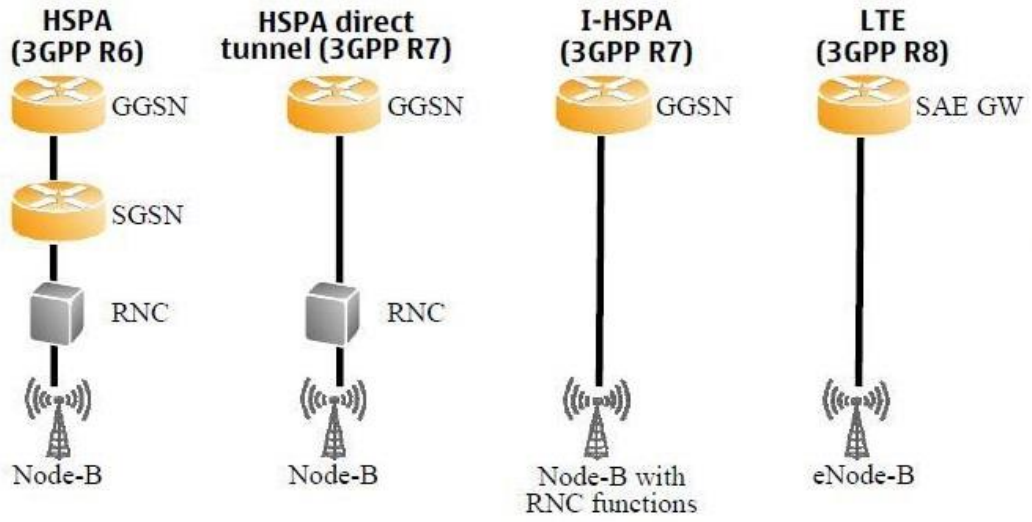

Figure 1.3 Evolution of network architecture

1.1.2 Heterogeneous Networks

Wireless cellular networks are typically deployed as homogeneous networks using a macro-centric planning process. A homogeneous cellular system is a network of base stations in a planned layout and a collection of user terminals, in which all the base stations have similar transmit power levels,

antenna patterns, receiver noise floors and similar backhaul connectivity to the (packet) data network. All base stations offer unrestricted access to user terminals in the network, and serve roughly the same number of user terminals, all of which carry similar data flows with similar QoS requirements [2].

Macro base station locations are carefully chosen through network planning, and the base station settings are properly configured to maximize the coverage and control the interference between base stations. As the traffic demand grows and the RF environment changes, the network relies on cell splitting or additional carriers to overcome capacity and link budget limitations and maintain uniform user experience. However, this deployment process is complex and iterative. Site acquisition for macro base stations with towers becomes more difficult in dense urban areas. A more flexible deployment model is needed for operators to improve broadband user experience in a ubiquitous and cost-effective way [2].

Typically, base stations are envisioned as big high-power towers or cell sites. And indeed, many are. Fundamentally, though, a BS must do three things. First, it must be able to initiate and accommodate spontaneous requests for communication channels with mobile users in its coverage area. Second, it must provide a reliable backhaul connection into the core network. This connection often is, but need not be, wired, but if wireless (possibly to another wired-in BS), it must not be in the same spectrum used for communication with the mobile users; otherwise, such a device should be considered a *relay*. Relays may be useful in some cases for coverage enhancement, but by reusing the same scarce "access" spectrum for backhaul, are inherently inferior to BSs. And third, BSs need to have a sustainable power source. Usually, this is a traditional wired power connection, but it could in principle be solar, scavenging, wind-powered, fossil fuel generated (e.g., "mobile access points, APs" in vehicles), or something else [3].

It is important to recognize that traditional tower-mounted BSs (what is known as macrocells) are just a single type of BS, albeit the backbone that has enabled cellular success to date. However, in many important markets, adding further macrocells is not viable due to cost and the lack of available sites; for example, many cities or neighbourhood associations are simply not very cooperative about opening up new tower locations. The problem facing operators is not coverage (which is now nearly universal) but capacity. There are just too many mobile users demanding too much data [3].

Evolution in wireless cellular systems have reached the point where an isolated system (with just one base station) achieves near optimal performance, as determined by information theoretic capacity limits. Future gains of wireless networks will be obtained more from advanced network topology, which will bring the network closer to the mobile users. Heterogeneous networks, utilizing a diverse set of base stations, can be deployed to improve spectral efficiency per unit area [2].

An obvious change in a HetNet (Heterogeneous Network) is the placement of base stations and their corresponding coverage or association regions. Whereas macrocells are generally somewhat evenly

spaced, they have most commonly been modelled as lying on a lattice, in particular a hexagonal grid. The association regions are then simply the corresponding hexagons. Smaller base stations are not regularly spaced, nor are their association regions homogeneous. Rather, they are scattered or clustered within the existing macrocell network and form their own embedded association regions, which are generally smaller, especially for the downlink, because the transmit power is significantly less. For example, typical macro, pico, and femto transmit powers are on the order of P_t = 40 W (effectively even higher due to high antenna gain), 2 W, and 100 mW. Thus, about an order of magnitude separates the transmit power of each tier of base stations, and their nominal downlink association areas vary by about the same amount. If a simple path loss model is used for average received power ($P_r = P_t d^{-\alpha}$), it can easily be shown that the cell area increases as $P_t^{\alpha/2}$, but it is in reality closer to linear given that mounting heights and antenna gains are larger for higher-power BSs; thus, they have effectively larger coverage areas [3]

Low-power base stations can be deployed to eliminate coverage holes in the macro-only system and improve capacity in hot spots. While the placement of macro base stations in a cellular network is generally based on careful network planning, the placement of pico/relay base stations may be more or less ad hoc, based on just a rough knowledge of coverage issues and traffic density (hot spots) in the network. Due to their lower transmit power and smaller physical size, pico/femto/relay base stations can offer flexible site acquisitions. Relay base stations offer additional flexibility in backhaul where wireline backhaul is unavailable or not economical [2].

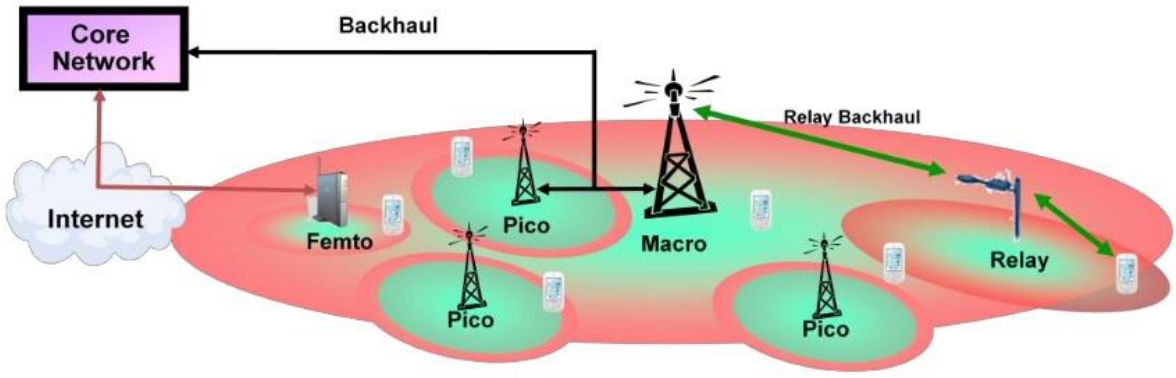

Figure 1.4 Heterogeneous Network using a mix of macro, pico, femto and relay bs

In a homogeneous network, each mobile terminal is served by the base stations with the strongest signal strength, while the unwanted signals received from other base stations are usually treated as interference. In a heterogeneous network, such principles can lead to significantly suboptimal performance. In such systems, smarter resource coordination among base stations, better server selection strategies and more advanced techniques for efficient interference management can provide substantial gains in throughput and user experience as compared to a conventional approach of deploying cellular network infrastructure [2].

Spatial modelling of the BS locations in a HetNet remains an open topic, since little information is yet available about picocell or femtocell deployments. It does seem clear that the grid-based models of the past are not scalable to an accurate model of a multitier HetNet, although one could construct a series of overlapping grids of differing densities. For example, in [4], macrocells are modelled with a hexagonal grid, with exactly six picocell BSs per macrocell, which are each located precisely on the boundaries between neighbouring BSs (Figure 1.5). Needless to say, such a setup is highly idealized. In the absence of prior information, the best statistical model is a uniform distribution, which in the two-dimensional plane corresponds to a Poisson point process. Such a spatial distribution for BS locations corresponds to complete randomness, whereas the grid provides no randomness. Thus, they are philosophically opposite, and any plausible HetNet BS deployment is bounded between these two extremes [3].

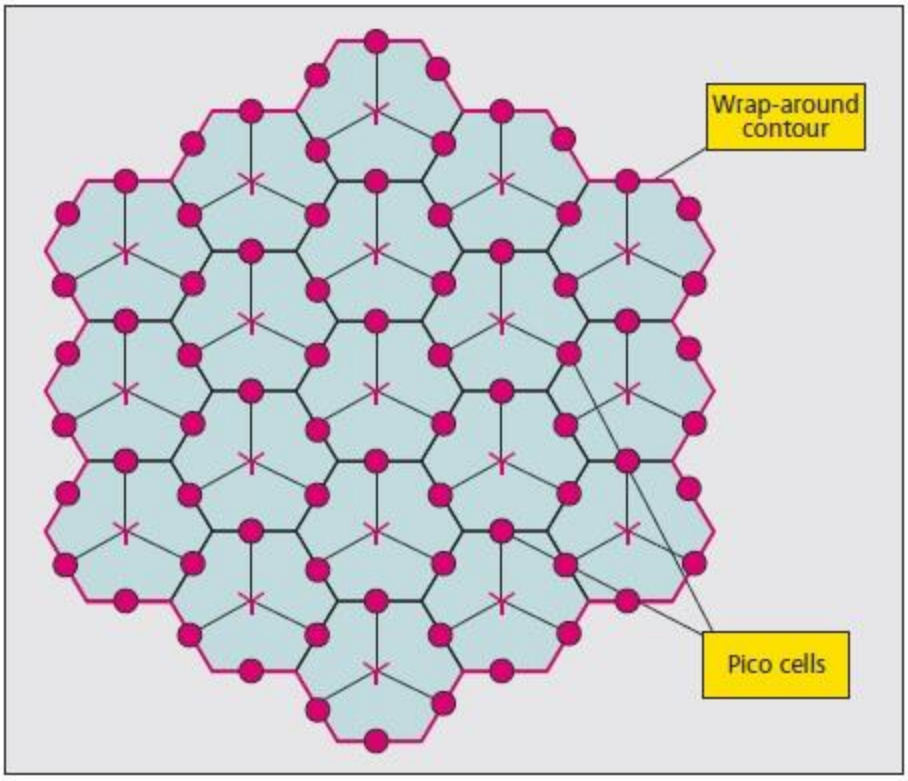

Figure 1.5 macro-pico model used by 3GPP in [4]

Even if the relative merits of the deterministic and Poisson models are open to debate, one important difference is that of tractability. Although the grid model is familiar, popular, and easy to conceptualize, it is not tractable. Distributions on rate, SINR, and other metrics are found through detailed system-level simulations that model nearby BSs as interference sources, and typically ignore more distant BSs. As small cells are added to the mix and the number of nearby interferers grows, the complexity of such simulations will also grow. Currently, the simulation of interference in such networks and the accurate determination of the SINR statistics under network dynamics is very time-intensive [3].

Contrarily, the Poisson model is surprisingly tractable, and a large class of powerful results and analytical tools are available from the field of stochastic geometry [5]. Because of the presumed independence between BS locations, SINR distributions can be obtained in closed form even for networks with an arbitrary number of BS types where each class of BS is distinguished with different transmit powers, densities (average number of BSs per unit area), and SINR targets [6] [3].

The pico base station is characterized by a substantially lower transmit power as compared to a macro base station, and a mostly ad hoc placement in the network. Because of unplanned deployment, most cellular networks with pico base stations can be expected to have large areas with low signal-to-interference conditions, resulting in a challenging RF environment for control channel transmissions to users on the cell edge. More importantly, the potentially large disparity (e.g. 20dB) between the transmit power levels of macro and pico base stations implies that in a mixed macro/pico deployment, the downlink coverage of a pico base station is much smaller than that of a macro base station [2].

This is not the case for the uplink, where the strength of the signal received from a user terminal depends on the terminal transmit power, which is the same for all uplinks from the terminal to different base stations. Hence, the uplink coverage of all the base stations is similar and the uplink handover boundaries are determined based on channel gains. This can create a mismatch between downlink and uplink handover boundaries, and make the base station-to-user terminal association (or server selection) more difficult in heterogeneous networks, compared to homogenous networks, where downlink and uplink handover boundaries are more closely matched [2].

If server selection is predominantly based on downlink signal strength, as in LTE Rel-8, the usefulness of pico base stations will be greatly diminished. In this scenario, the larger coverage of high-power base stations limits the benefits of cell splitting by attracting most user terminals towards macro base stations based on signal strength without having enough macro base station resources to efficiently serve these user terminals. And lower power base-stations may not be serving any user terminals [2].

Even if all the low-power base stations can use available spectrum to serve at least one user terminal, the difference between the loadings of different base stations can result in an unfair distribution of data rates and uneven user experiences among the user terminals in the network. Therefore, from the point of view of network capacity, it is desirable to balance the load between macro and pico base stations by expanding the coverage of pico base stations and subsequently increase cell splitting gains. This concept is referred to as range expansion, which is illustrated in Figure 1.6 [2].

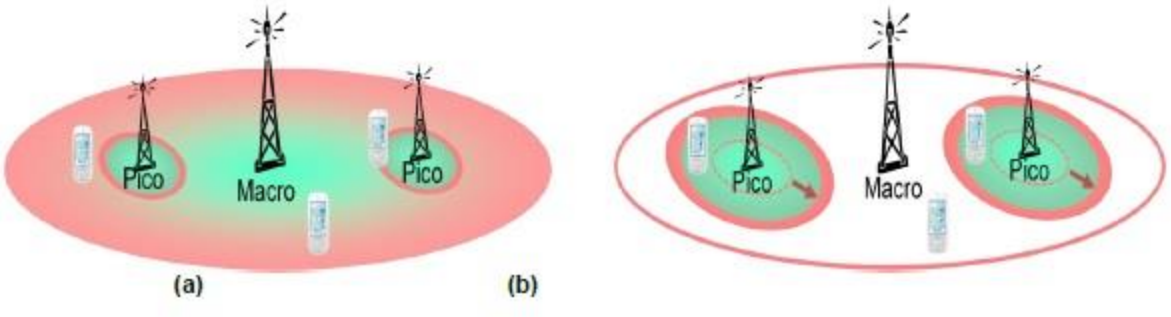

Figure 1.6 (a) Limited footprint of picos due to strong macro signal;

(b) Increased footprint of picos with range expansion

Inter-cell Interference Coordination

In a heterogeneous network with range expansion, in order for a user terminal to obtain service from a low-power base station in the presence of macro base stations with stronger downlink signal strength, the pico base station needs to perform both control channel and data channel interference coordination with the dominant macro interferers and the user terminals need to support advanced receivers for interference cancellation. In the case of femto base stations, only the owner or subscribers of the femto base-station may be allowed to access the femto base stations [2].

For user terminals that are close to these femto base stations but yet barred from accessing them, the interference caused by the femto base stations to the user terminals can be particularly severe, making it difficult to establish a reliable downlink communication to these user terminals. Hence, as opposed to homogeneous networks, where resource reuse (with minor adjustments) is a good transmission scheme, femto networks necessitate more coordination via resource partitioning across base stations to manage inter-cell interference [2].

As a result, Inter-cell Interference Coordination (ICIC) is critical to heterogeneous network deployment. A basic ICIC technique involves resource coordination amongst interfering base stations, where an interfering base station gives up use of some resources in order to enable control and data transmissions to the victim user terminal. More generally, interfering base stations can coordinate on transmission powers and/or spatial beams with each other in order to enable control and data transmissions to their corresponding user terminals [2].

Resource partitioning can be performed in time domain, frequency domain, or spatial domain. Time domain partitioning can better adapt to user distribution and traffic load changes and is the most attractive method for spectrum-constrained markets. For example, a macro base station can choose to reserve some of the subframes in each radio frame for use by pico stations based on the number of

user terminals served by pico and macro base stations and/or based on the data rate requirements of the user terminals [2].

Figure 1.7 shows an example of time domain partitioning between macro and pico. Frequency domain partitioning offers less granular resource allocation and flexibility, but is a viable method, especially in an asynchronous network. Spatial domain partitioning can be supported by Coordinated Multipoint Transmission (CoMP), which is further studied in 3GPP Rel-11 [2].

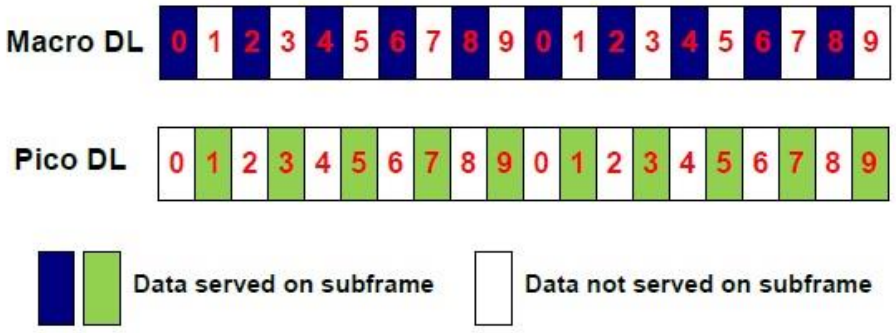

Figure 1.7 Time domain resource partitioning between macro and pico DL: 50% for each

Using time-domain resource partitioning, a macro base-station can use almost blank subframes (ABSF) to reserve some subframes for pico. The macro base-station keeps transmitting legacy common control channels during ABSFs to enable full backward compatibility with legacy user terminals. The user terminals can cancel interference on common control channels of ABSF caused either by higher power macro stations or by close-by femto stations that the user terminals are prohibited to access. The function of the advanced receiver is illustrated in Figure 1.8. The interference cancellation receiver fully handles colliding and non-colliding Reference Signal (RS) scenarios and removes the need for cell planning of heterogeneous deployment [2].

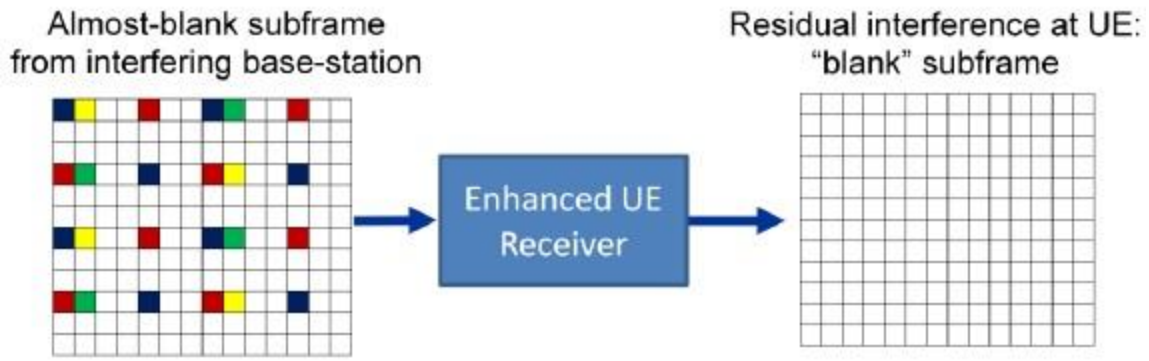

Figure 1.8 Advanced user equipment receiver cancels the reference signal in almost-blank subframes from interfering base stations

Slowly-Adaptive Interference Management

Using this approach, resources are negotiated and allocated over time scales that are much larger than the scheduling intervals. The goal of the slowly-adaptive resource coordination algorithm is to find a combination of transmit powers for all the transmitting base stations and user terminals, and over all the time and/or frequency resources that maximizes the total utility of the network. The utility can be defined as a function of user data rates, delays of QoS flows, and fairness metrics [2].

Such an algorithm can be computed by a central entity that has access to all the required information for solving the optimization problem, and has control over all the transmitting entities. Such a central entity may not be available or desirable in most cases for several reasons, including the computational complexity as well as delay or bandwidth limitations of the communication links that carry channel information or resource usage decisions. As a result, a distributed algorithm that makes resource usage decisions based on the channel information only from a certain subset of nodes may be more desirable [2].

The coordination can be performed via the backhaul (X2 interface in LTE). For example, pico stations can send load information and resource partitioning request to macro stations using X2 messages, while macro stations send resource partitioning response and update back to pico stations [2].

1.2 Motivation and Objectives

To cope with the increased demand for wireless services the operators are considering heterogeneous systems, i.e., the deployment of small-cells within the boundaries of the existing macro-cells and sharing the same spectrum [7]. This requires the development of efficient interference management techniques because if not carefully designed the small-cells signals may generate harmful interference on the macro-cell [8]. As the macro-cell is the licensee (the owner of the spectrum license) to deal with the interference problem, small-cells must reuse the unused macro-cell resources. Active use of the spatial domain through multiple antenna techniques is of outmost importance to minimize the interference level in a heterogeneous network environment. Interference alignment (IA) is a precoding technique that is able to achieve the maximum degrees of freedom of the interference channel, in a variety of settings [9]. IA works by dividing the receiver space in two parts, one for interference and the other for the intended signal. Closed form solutions for IA are only available for some specific cases [10]. For the other cases, iterative methods may be considered, using for example a convergent alternating minimization approach [11]. IA techniques were recently proposed to mitigate the interference of small-cell user terminals (UTs) towards the macro-cell BS [12][13]. In [12] the authors proposed a new interference alignment scheme that successively creates transmit beam-forming vectors for the small-cell terminals and for the macro BS assuming that they have different number

of transmit antennas. The work in [13] studied several IA techniques with different levels of inter-system information sharing.

Single carrier frequency division multiple access (SC-FDMA) is a promising solution technique for high data rate uplink communications in future cellular systems. The principal advantage of SC-FDMA is the peak-to-average power ratio (PAPR), which is lower than that of OFDMA [14]. SC-FDMA was adopted for the uplink, as a multiple access scheme, of the current long-term evolution (LTE) cellular system [1]. Single-carrier frequency domain equalization (SC-FDE) is widely recognized as an excellent alternative to OFDM, especially for the uplink of broadband wireless systems [15]. For this reason, there has been significant interest in the design of nonlinear FDE in general and decision feedback FDE in particular, with the iterative block decision feedback equalizer (IB-DFE) being the most promising nonlinear FDE [16].

The aim of this work is to design iterative frequency domain equalizers based on the IB-DFE principle, for SC-FDMA based heterogeneous networks, in order to efficiently separate the spatial streams at both macro base station (BS) and the central unit (CU). We assume that the macro-cell defines an interference subspace where other systems are allowed to transmit information without causing any interference. All small-cells align their transmission along this subspace so that no interference is generated at the macro-cell. The proposed receiver structures are explicitly designed taking into account inter-system and residual inter-carrier (IC) interferences, allowing an efficient co-existence of both systems.

1.3 Contributions

The main results of this work were recently published in an international conference.

J. Assunção, D. Castanheira, F. Oliveira, A. Silva, R. Dinis, A. Gameiro, "IA-Precoding with IB-DFE Scheme for Uplink SC-FDMA Heterogeneous Networks", in proceedings of International Conference on Wireless and Mobile Communications Systems (WMCS'14), Lisbon, Portugal

1.4 Outline

Starting with a small introduction on how the mobile systems evolved to the LTE system used today, a brief introduction into heterogeneous networks, the motivation and objectives, we present the following chapters:

In chapter 2, it is presented the OFDMA and SC-FDMA multicarrier systems, as well as MIMO techniques. Some of their characteristics will be overviewed as well as some useful techniques against interference such as orthogonality and the introduction of a cyclic prefix. In the MIMO section, the three multiple antenna formats will be discussed, the different types of diversity and spatial multiplexing.

In chapter 3, it is studied the interference alignment (IA) and the iterative equalization concepts. Some of the applications of interference alignment are presented such as X networks for single and multiple antenna nodes. After that, iterative equalization for single carrier systems is presented, focusing on IB-DFE concept.

In chapter 4, it is proposed the IB-DFE PIC based receiver structure with IA-precoded SC-FDMA systems on a heterogeneous network. The signal processing will be studied in some detail at the receiver and the transmitter. The performance of the proposed scheme will be analysed and compared using different parameters.

In the last chapter, work conclusions are presented and some possible future research guidelines presented.

Notations: Boldface capital letters denote matrices and boldface lowercase letters denote column vectors. The operations $(.)^H$ and tr(.) represent the Hermitian transpose and the trace of a matrix. $\{\alpha_l\}_{l=1}^{L}$ represents a L length sequence. $\mathbf{I}_N$ is the identity matrix with size $N \times N$. $\mathcal{N}(\mathbf{A})$ denotes a matrix whose columns span the null space of matrix $\mathbf{A}$. The indexes *s* and *p* are used to represent the small-cell/secondary and the macro-cell/primary systems, respectively.

2. Wireless Transmission Techniques

In a single carrier transmission, the information is modulated in only one carrier, adjusting phase, amplitude or frequency. A high data rate, a high symbol rate, in a digital system means that the bandwidth use is also high. In multicarrier transmission, the transmitted data is divided into many sub streams which are sent through many different subchannels. In ideal conditions these channels would be orthogonal. Because of this division in the high data rate, each subchannel will have a much lower than the total data rate, leading to a much lower bandwidth. The number of subchannels is chosen so that each subchannel has a bandwidth smaller than the coherence bandwidth. The subchannels don't need to be contiguous, being efficiently implemented digitally. Some multicarrier systems like OFDM/A and SC-FDMA will be presented in this chapter.

The growing demand for higher data rates with better quality of service (QoS) require more than the techniques presented at the start of this chapter. Multiple antennas at the transmitters and receivers became an innovative technique that promised higher data rates at larger distances with consuming extra bandwidth or transmit power. Some of those multi-antenna formats are shown here.

2.1 OFDM/A

OFDM has become one of the most exciting developments in the area of modern broadband wireless networks. Although the notion of multicarrier transmission or multiplexing can be dated back to the 1950, high spectral efficiency and low cost implementation of FDM became possible in the 1970s and 1980s with advances in Digital Fourier Transform (DFT). It is not until the 1990s that we witnessed the first commercial OFDM -based wireless system- the digital broadcasting (DAB) standard [17].

Despite being an almost 50 year old concept, OFDM only became the main choice for wireless applications in the last decade. One of the biggest advantages of OFDM is the ability to convert dispersive broadband channels into parallel narrowband sub-channels, significantly simplifying equalization at the receiver end. Another feature of OFDM is the flexibility in allocating power and rate optimally among broadband sub-carriers. It's an ability particularly important in broadband wireless where multi-path channels are frequency-selective [17].

The arrival time of scattered multipath signals are inevitably distinct. Whether these delays smear the transmitted signal depends on the product of the signal bandwidth and the maximal differential delay spread as show in Figure 2.1 [17].

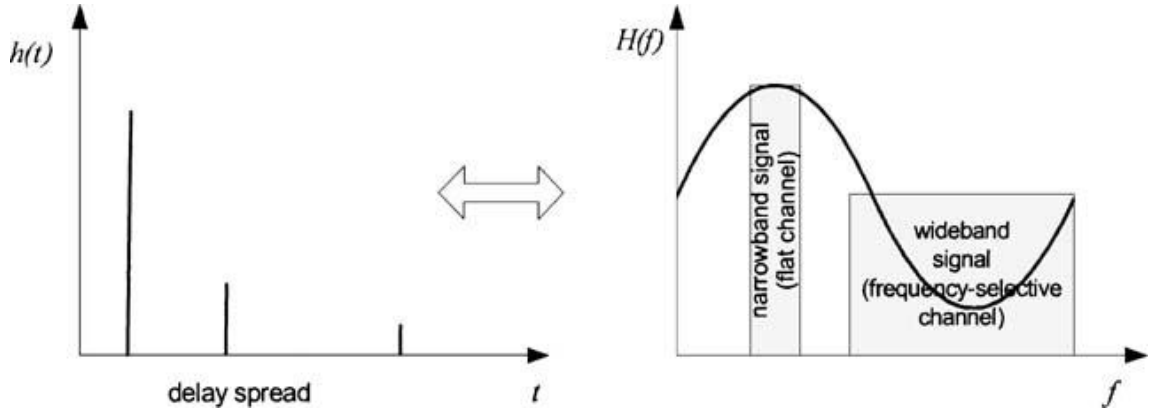

Figure 2.1 Time Dispersive Channel

The short-term fluctuation of the received signal in time domain can be explained by the Doppler effects due to the movement of the transmitter, the receiver, or the environment. The Doppler Effect is multiplicative in time, rendering the channel impulse response linear, but time variant [17].

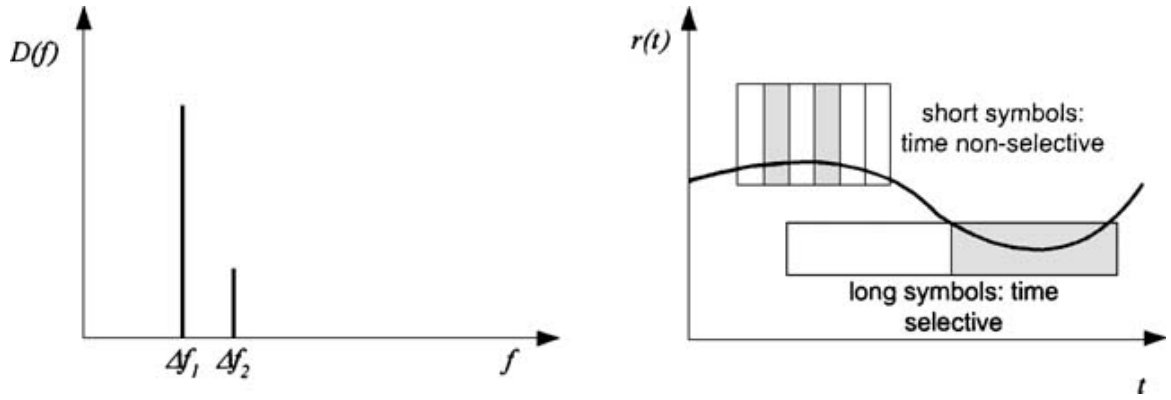

Figure 2.2 Frequency Dispersive Channel

Multipath induced intersymbol interference is usually handled by equalizers at the receiver side. On the other hand, if the signal waveform is designed to be immune to multipath distortions, the receiver can be drastically simplified. In order to maintain the integrity of the waveform while preventing intersymbol interference a cyclic prefix can be used at the transmitter. As shown in Figure 2.3, any multipath component with delays less or equal to the guard period will maintain their complex exponential waveforms within the observation window, leading to an intact signal waveform at the receiver [17].

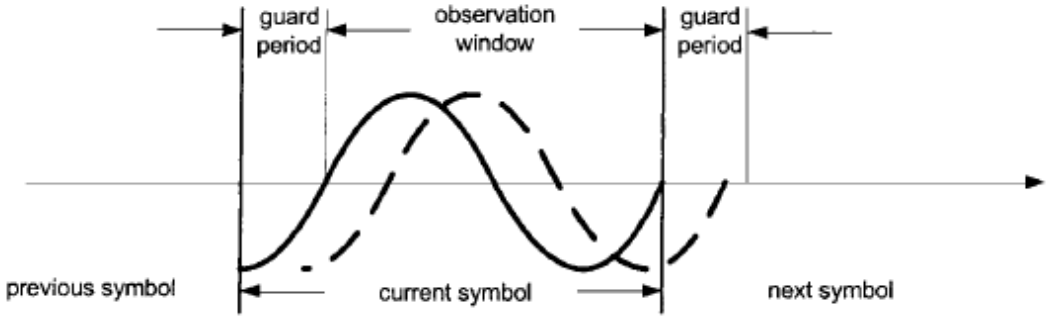

Figure 2.3 Cyclic Prefix Guard Interval

While the CP (Cyclic Prefix) in FDM reduces the multipath channel effect to a scalar on each sub-channel, signals across different sub-channels must not interfere with each other. For two waveforms to be orthogonal within [0,T], they must be separated by 1/T hertz. The FDM that satisfies such frequency requirement is referred to as OFDM – orthogonal frequency division multiplexing. Each tone in OFDM is referred to as a sub-carrier. The typical spectrum of OFDM signals is shown in Figure 2.4. The overlapping sinc shaped spectrum assure zero inter-sub-channel interference at the right frequency sampling points [17].

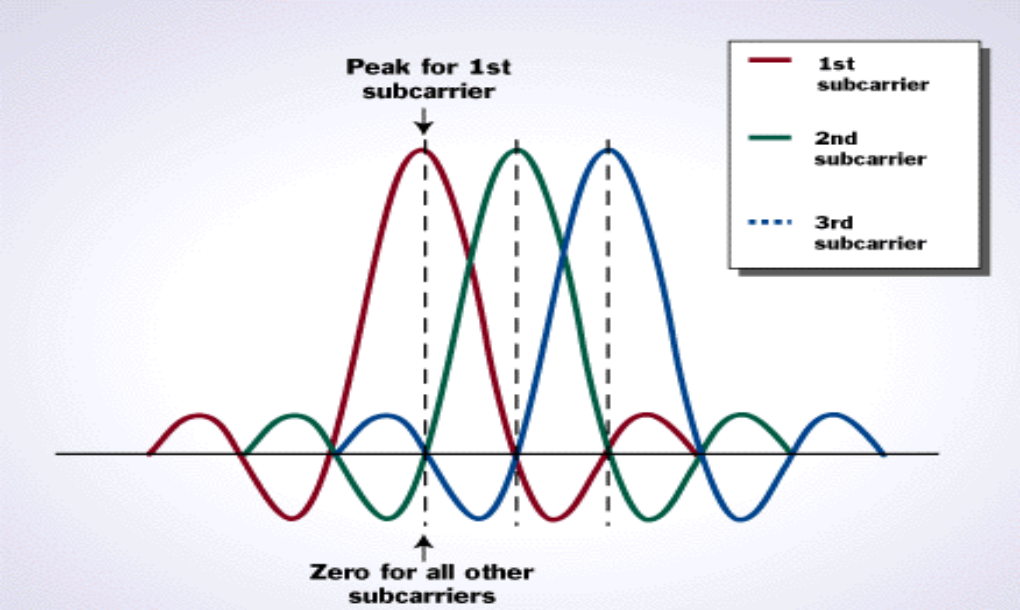

Figure 2.4 OFDM Spectrum

A typical transmitter and receiver of an OFDM chain can be seen in Figure 2.5. Unlike signal-carrier modulation, OFDM is performed on a block by block basis. At the transmitter, a block of information symbols are first converted from serial to parallel into K subcarriers. The orthogonal modulation is carried out using an inverse FFT followed by a parallel to serial conversion. After the converter, the last L points are appended to the beginning of the sequence as the cycle prefix. The resulting samples are then shaped and transmitted. Each transmitted block is known as an OFDM symbol [17].

On the receiver side the process is reversed using an FFT operation. The sampled signals are first processed to find the starting point of a block and the proper demodulation window. After removing the CP, the signal is converted from serial to parallel and delivered to the FFT. The result are symbols modulated on the K sub-carriers, each multiplied by a complex channel gain. Different demodulation/decoding schemes are then used to recover the information depending on the channel information [17].

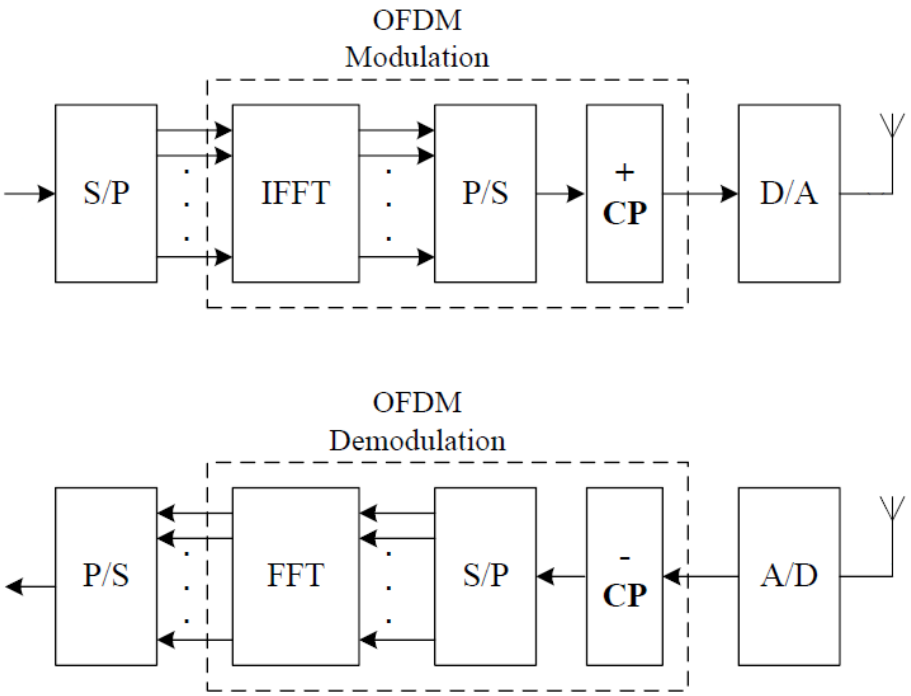

Figure 2.5 OFDM Block diagram

"An OFDMA system is defined as one in which each terminal occupies a subset of carriers (termed an OFDMA traffic channel), and each traffic channel is assigned exclusively to one user at any time" [18].

OFDMA could only be accomplished using multiple analogue RF modules if one terminal occupied multiple frequency bands. With the rise of OFDM, FDMA gained a new life as a broadband multiple access scheme. The use of IFFT/FFT allowed terminals to arbitrarily combine multiple frequencies at the baseband, resulting in orthogonal frequency division multiple access scheme shown as figure 2.6

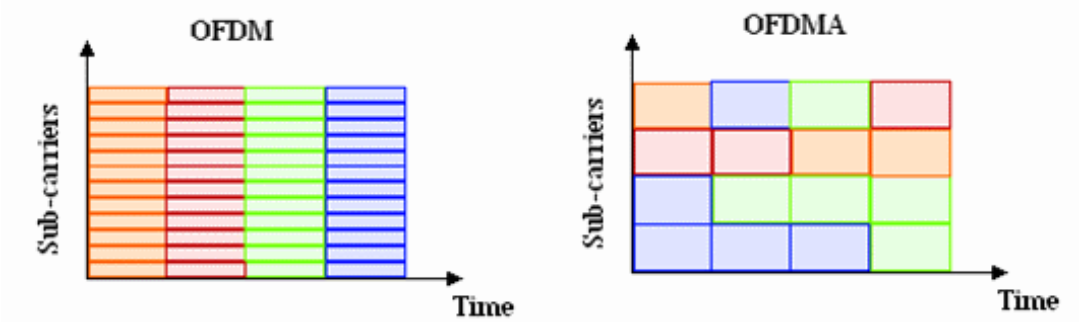

Figure 2.6 OFDM/OFDM in frequency and time domain

In OFDMA, there is no overlap in the frequency domain at any given time. The bands assigned to any given user can change over time however.

LTE has several OFDMA bandwidth options of 1.4, 3, 5, 10, 15 or 20 MHz. Depending on which bandwidth use the spectrum can be divided into 128, 512, 1024 or 2048 subcarriers. In LTE-Advanced up to 5 carriers can be aggregated for larger bandwidth.

Applying the three types of channelization schemes to an OFDM network results in three types of systems: OFDM-TDMA, OFDM-CDMA (also known as MC-CDMA) and OFDMA. OFDM-TDMA and MC-CDMA are more flexible, given that the number of slots or codes that can be assigned to each user are adjustable, resulting in different data rates. When it comes to real system operations, OFDMA is clearly advantageous [17].

2.1.1 Granularity

Early broadband access systems utilize OFDM-TDMA to offer a straightforward way of multiple-accessing: each user uses a small number of OFDM symbols in a time slot and, multiple users share the radio channel through TDMA. The method has two obvious shortcomings. First, every time a user utilizes the channel, it has to burst its data over the entire bandwidth, leading to a high peak power and therefore low RF efficiency. Second, when the number of sharing users is large, the TDMA access delay can be excessive. OFDMA is a much more flexible and powerful way to achieve multiple-access with OFDM modem. In OFDMA, the multiple-access is not only supported in the time domain, but also in the frequency domain, just like traditional FDMA minus the guard-band overhead. As a result, an OFDMA system can support more users with much less delay. The finer data rate granularity in OFDMA, as illustrated in Figure 2.7**,** is paramount to rich media applications with diverse QoS requirements [17].

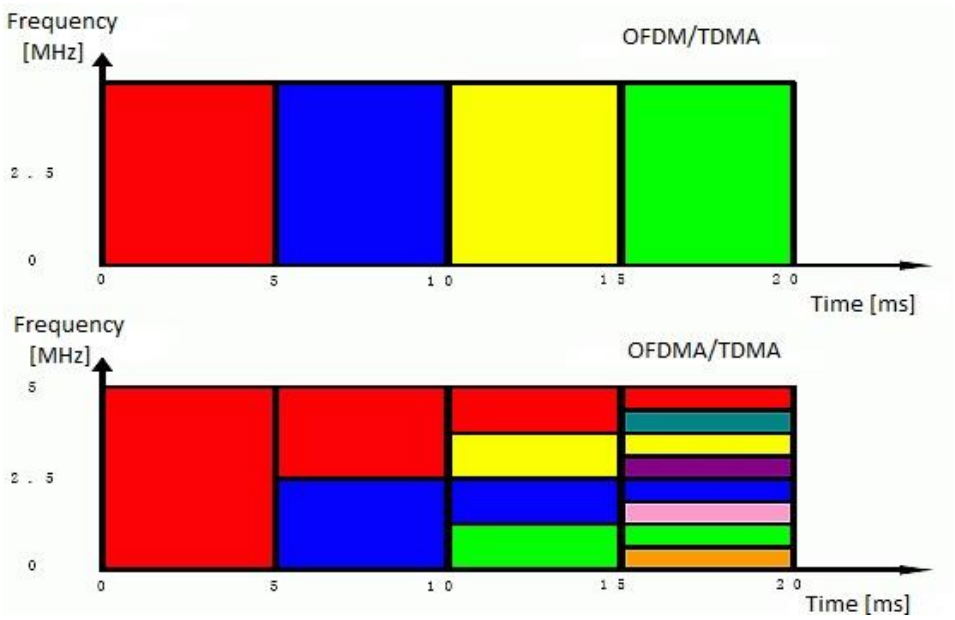

Figure 2.7 Resource Partitioning in OFDMA

2.1.2 Link budget

Since each TDMA user must burst its data over the entire bandwidth during the allocated time slots, the instantaneous transmission power (dictated by the peak rate) is the same for all users, regardless of their actual data rates. This inevitably creates a link budget deficit that handicaps the low rate users. Unlike TDMA, an OFDMA system can accommodate a low-rate user by allocating only a small portion of its band (proportional to the requested rate). For example, by reducing the effective transmit bandwidth to 1/64 of the system bandwidth, OFDMA can provide an about 18 dB uplink budget advantage over OFDM-TDMA [17].

2.1.3 Receiver simplicity

OFDMA has the merit of easy decoding at the receiver side, as it eliminates the intra-cell interference avoiding CDMA type of multi-user detection. This is not the case in MC-CDMA, even if the codes are designed to be orthogonal. Users' signals can only be detected jointly since the code orthogonality is destroyed by the frequency selective fading. The fact that users' channel characteristics must be estimated also favours OFDMA. In MC-CDMA, users' channel responses must be estimated using complex jointly estimation algorithms. Furthermore, OFDMA is the least sensitive multiple access scheme to system imperfections [19] [17].

2.1.4 Multiuser diversity

Broadband signals experience frequency selective fadings. The frequency response of the channel varies over the whole frequency spectrum. The fact that each user has to transmit its signal over the entire spectrum in OFDM-TDMA/CDMA leads to an averaged-down effect in the presence of deep fading and narrowband interference. On the other hand, OFDMA allows different users to transmit over different portions of the broadband spectrum (traffic channel). Since different users perceive different channel qualities, a deep faded channel for one user may still be favourable to others. Therefore, through judicious channel allocation, the system can potentially outperform interference-averaging techniques by a factor of 2 to 3 in spectrum efficiency [20] [17].

2.2 SC-FDMA

High PAPR (Peak-to-Average Power Ratio) associated with OFDM forced 3GPP to find a different modulation scheme for the uplink in LTE. SC-FDMA was chosen since it combines the low PAPR techniques of single-carrier transmission systems with the multipath resistance and flexible allocation of OFDMA.

Data symbols in the time domain are converted to the frequency domain using a DFT (Discrete Fourier Transform). Once in the frequency domain they are mapped to the desired location in the overall channel bandwidth before being converted back to the time domain using IFFT (Inverse FFT). Finally, the CP (Cycle Prefix) is inserted. SC-FDMA is also called Discrete Fourier Transformation Spread OFDM (DFT-S-OFDM) because of the involved process [21].

A graphical comparison of OFDMA and SC-FDMA is helpful to understand the differences between these two modulation schemes. In figure 2.8 an example is given with 4 subcarriers.

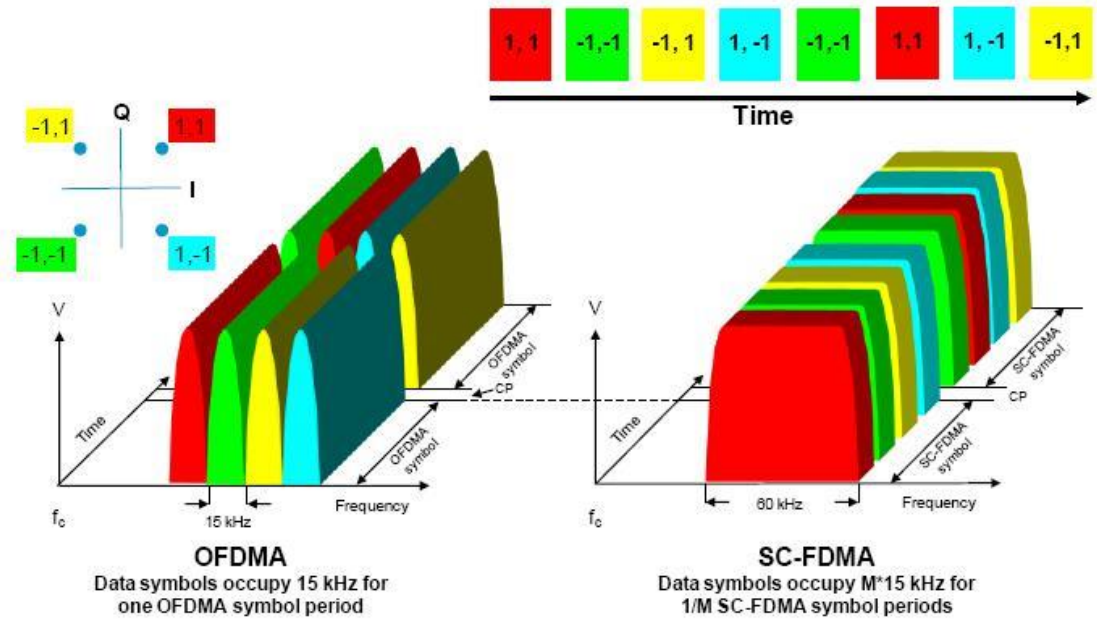

Figure 2.8 Comparison between OFDMA and SC-FDMA

On the left side of figure 2.8 adjacent 15 KHz subcarriers – already positioned at the desired place in the channel bandwidth – are each modulated for the OFDMA symbol period of 66.7 µs by one QPSK data symbol. In this four subcarrier example, four symbols are taken in parallel. These are QPSK data symbols so only the phase of each subcarrier is modulated and the subcarrier power remains constant between symbols. After one OFDMA symbol period has elapsed, The CP is inserted and the next four symbols are transmitted in parallel. The CP is shown as a gap in the figure, but it is actually used a copy of the end of the next symbol maintaining a continuous transmission power with a phase discontinuity at the symbol boundary. An IFFT is performed on each subcarrier to create *N* time-domain signals which, in turn are vector-summed to create the final time-domain waveform used for transmission [21].

In SC-FDMA, however, signal generation begins with a special precoding process, but then continues in a manner similar to OFDMA. The most obvious difference between the two schemes is that OFDMA transmits the four QPSK data symbols in parallel, one per subcarrier, while SC-FDMA

transmits the four QPSK data symbols in series at four times the rate, with each symbol occupying a wider 4 x 15 KHz bandwidth [21].

On a visual comparison, the OFDMA signal is clearly multi-carrier with one data symbol per subcarrier, while the SC-FDMA signal appears to be more like a single-carrier (thus the SC in the SC-FDMA name) with each data symbol being represented by one wide signal. OFDMA and SC-FDMA symbol lengths are the same at 66.7 µs, however the SC-FDMA symbol contains *N* sub-symbols that represent the modulating data. It is the parallel transmission of multiple symbols that creates the undesirable high PAPR of OFDMA. Since *N* data symbols are transmitted in series at *N* times the rate, SC-FDMA occupied bandwidth is the same as multi-carrier OFDMA, but with the advantage of having the same PAPR as used for the original data symbols. Joining many narrowband QPSK waveforms in OFDMA will always create higher peaks than would be seen in the wider-bandwidth, single-carrier QPSK waveform of SC-FDMA. As the number of subcarriers increases, the PAPR of OFDMA with random modulating data approaches Gaussian noise statistics, while regardless of the value of N, PAPR in SC-FDMA remains the same as that used for the original data symbols [21].

SC-FDMA signal creation begins with a special precoding process. Figure 2.9 shows how it starts, creating a time-domain waveform of the QPSK data sub-symbols. Using the four color-coded QPSK data symbols, the process creates one SC-FDMA symbol in the time-domain by computing the trajectory traced by moving from one QPSK data symbol to the next. This computation is done at N times the rate of the SC-FDMA symbol such that one SC-FDMA symbol contains *N* consecutive QPSK data symbols. Time-domain filtering of the data symbol transitions occurs in any real implementation [21].

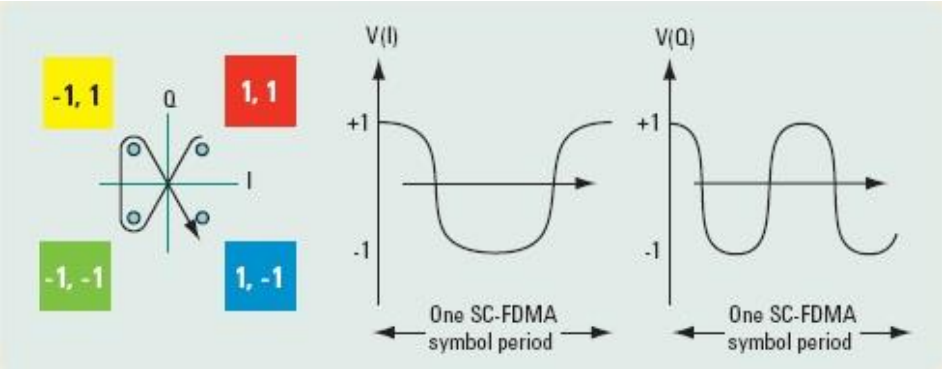

Figure 2.9 Creating time-domain waveform of SC-FDMA symbol

Once the IQ representation of one SC-FDMA symbol has been created in the time-domain, the next step is to represent that symbol in the frequency domain by using a DFT. The DFT sampling frequency is chosen such that the time-domain waveform of one SC-FDMA symbol is fully represented by *N*-DFT bins spaced 15 KHz apart, with each bin representing one subcarrier in which amplitude and phase are held constant for 66.7 µs [21].

A one-to-one correlation exists between the number of data symbols to be transmitted during one SC-FDMA symbol period and the number of DFT bins created. This becomes the number of occupied subcarriers. When an increased number of data symbols are transmitted during one SC-FDMA period, the waveform changes faster, generating a higher bandwidth, therefore requiring more DFT bins to represent the signal in the frequency domain [21].

The signal generation process continues with the shift in the baseband DFT representation of the time-domain SC-FDMA symbol to the desired part of the overall channel bandwidth. Since the signal is now represented as a DFT, frequency-shifting is a simple process achieved by copying the *N* bins into a larger DFT space. This larger space equals the size of the system cannel bandwidth, of which there are six in LTE, from 1.4 to 20 MHz. The SC-FDMA signal, which is usually narrower than the channel bandwidth, can be positioned anywhere in the channel bandwidth, thus executing the Frequency Division Multiple Access (FDMA) essential for efficiently sharing the uplink between multiple users [21].

To complete the SC-FDMA signal generation, the process follows the same steps as OFDMA. Performing IDFT converts the frequency-shifted signal to the time-domain and inserting the CP provides the robustness of OFDMA against multipath [21].

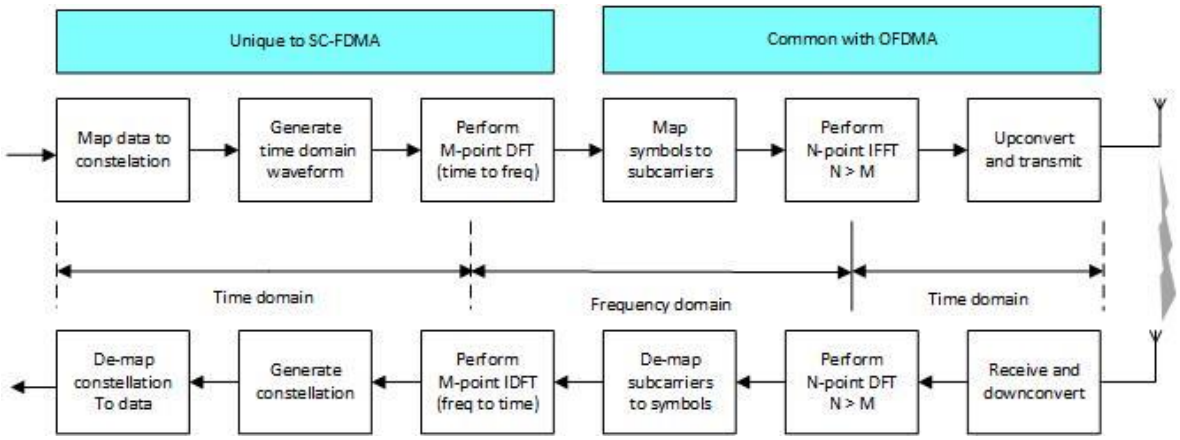

Figure 2.10 SC-FDMA and OFDMA signal generation

The question can be asked of how SC-FDMA can be resistant to multipath since the data symbols are still short. In OFDMA the modulating data symbols are constant over the 66.7 µs OFDMA symbol period, but an SC-FDMA symbol is not constant over time since it contains *N* sub-symbols of much shorter duration. The multipath resistance of the OFDMA demodulation process seems to rely on the long data symbols that map directly onto the subcarriers. Fortunately, it is the constant nature of each subcarrier, not the data symbols, that provides the resistance to delay spread. The DFT of the time-varying SC-FDMA symbol generated a set of DFT bins constant in time during the SC-FDMA symbol period, even while the modulating data symbols varied over the same period. It is inherent to the DFT

process that the time-varying SC-FDMA symbol is represented in the frequency domain by *N* time-invariant subcarriers. Thus, even SC-FDMA with its short data symbols benefits from multipath protection [21].

While it may seem counterintuitive that *N* time-invariant DFT bins can fully represent a time-varying signal, the DFT principle is simply illustrated by considering the sum of two fixed sine waves at different frequencies. The result is a non-sinusoidal time-varying signal, fully represented by two fixed sine waves [21].

The table in figure 2.14 summarizes the differences between the OFDMA and SC-FDMA modulation schemes. When OFDMA is analysed one subcarrier at a time, it resembles the original data symbols. At full bandwidth, the signal looks like Gaussian noise in terms of its PAPR statistics and the constellation. The opposite is true for SC-FDMA. In this case, the relationship to the original data symbols is evident when the entire signal bandwidth is analysed. The constellation (and PAPR) of the original data symbols can be observed rotating at *N* times the SC-FDMA symbol rate (seven percent reduction sue to adding CP). When analysed at the 15 KHz subcarrier spacing, the SC-FDMA PAPR and constellation are meaningless because they are *N* times narrower than the information bandwidth of the data symbols [21].

Modulation format	OFDMA		SC-FDMA	
Analysis bandwidth	15 kHz	Signal BW (N x 15 kHz)	15 kHz	Signal BW (N x 15 kHz)
Peak-to-average power ratio	Same as data symbol	High PAR (Gaussian)	Not meaningful (< data symbol)	Same as data symbol
Observable IQ constellation	Same as data symbol at 66.7 µs rate	Not meaningful (Gaussian)	Not meaningful (< data symbol)	Same as data symbol at N x 66.7 µs rate

Figure 2.11 Analysis of OFDMA and SC-FDMA at different bandwidths

2.3 MIMO Systems

Using multiple antennas at the transmitter and receiver in wireless systems, popularly known as MIMO (multiple-input multiple-output) technology, has rapidly gained in popularity over the past decade due to its powerful performance-enhancing capabilities. Communication in wireless channels is impaired predominantly by multi-path fading. Multi-path is the arrival of the transmitted signal at an intended receiver through differing angles and/or differing time delays and/or differing frequency (i.e., Doppler) shifts due to the scattering of electromagnetic waves in the environment. Consequently,

the received signal power fluctuates in space (due to angle spread) and/or frequency (due to delay spread) and/or time (due to Doppler spread) through the random superposition of the impinging multi-path components. This random fluctuation in signal level, known as fading, can severely affect the quality and reliability of wireless communication. Additionally, the constraints posed by limited power and scarce frequency bandwidth make the task of designing high data rate, high reliability wireless communication systems extremely challenging [22].

The MIMO technology constitutes a breakthrough in wireless communication system design. The technology offers a number of benefits that help meet the challenges posed by both the impairments in the wireless channel as well as resource constraints. In addition to the time and frequency dimensions that are exploited in conventional single-antenna (single-input single-output) wireless systems, the leverages of MIMO are realized by exploiting the spatial dimension (provided by the multiple antennas at the transmitter and the receiver [22].

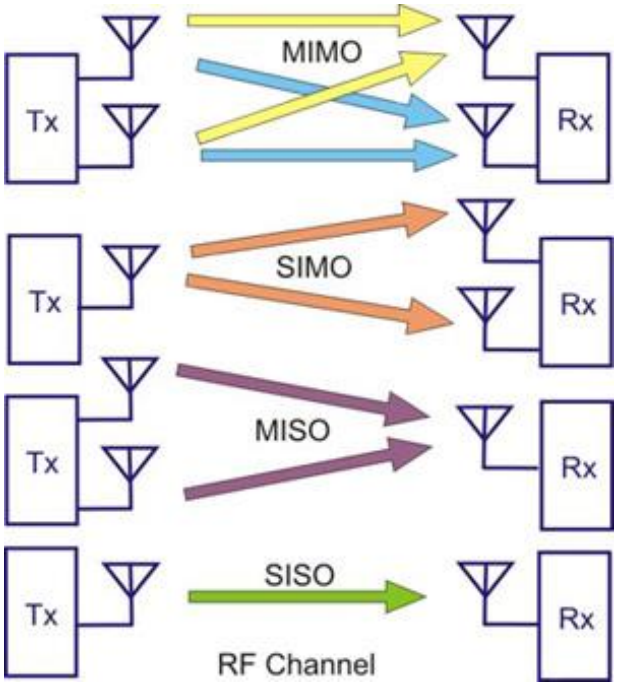

Figure 2.12 Multiple antenna configurations

MIMO technology has several benefits that help achieve significant performance gains. They are array gain, spatial diversity gain, spatial multiplexing gain and interference reduction.

2.3.1 Array gain

Array gain is the increase in receive SNR that results from a coherent combining effect of the wireless signals at a receiver. The coherent combining may be realized through spatial processing at the receive

antenna array and/or spatial pre-processing at the transmit antenna array. Array gain improves resistance to noise, thereby improving the coverage and the range of a wireless network [22].

2.3.2 Spatial diversity gain

As mentioned earlier, the signal level at a receiver in a wireless system fluctuates or fades. Spatial diversity gain mitigates fading and is realized by providing the receiver with multiple (ideally independent) copies of the transmitted signal in space, frequency or time. With an increasing number of independent copies (the number of copies is often referred to as the diversity order), the probability that at least one of the copies is not experiencing a deep fade increases, thereby improving the quality and reliability of reception. A MIMO channel with M_T transmit antennas and M_R receive antennas potentially offers $M_T M_R$ independently fading links, and hence a spatial diversity order of $M_T M_R$ [22].

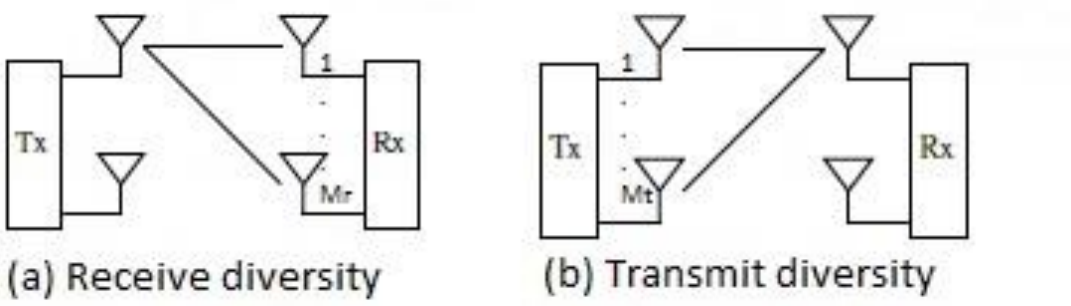

Figure 2.13 Receive and transmit diversity

In spatial diversity there are two different techniques whose use depends on the number of antennas available on the receiver and on the transmitter.

Receive diversity

Consider the arrangement in Figure 2.13(a). One transmit antenna at a node is sending to two receive antennas at a second node. This is known as a 1x2 system. Real systems may have more than two receive antennas, but two will suffice for our explanation. With this setup, each receive antenna receives a copy of the transmitted signal modified by the channel between the transmitter and itself. The channel gains h_{ij} are complex numbers that represent both the amplitude attenuation over the channel as well as the path dependent phase shift. The receiver measures the channel gains based on training fields in the packet preamble. Note that the gains differ for each subcarrier (in frequency-selective fading) as well as for each antenna. The question now is how to combine the two received signals to make best use of them [23].

Two diversity techniques are considered to show the extremes. The simplest method is to use the antenna with the strongest signal (hence the largest SNR) to receive the packet and ignore the others. We will call this method SEL, for selection combining. It helps with reliability, because both signals are unlikely to be bad, but it wastes perfectly good received power at the antennas that are not chosen [23].

The better method is to add the signals from the two antennas together. However, this cannot be done by simply superimposing their signals, or we will have just recreated the effects of multi-path fading. Rather, the signals should each be delayed until they are in the same phase; then, the power in the signals will combine coherently. To do this, the receiver needs a dedicated RF chain for each antenna to process the signals. This increases the hardware complexity and power consumption, but yields better performance [23].

As a twist in the above, the signals are also weighted by their SNRs. This gives less weight to a signal that has a larger fraction of noise, so that the effects of the noise are not amplified. The result is maximal-ratio combining, or MRC. MRC is known to be optimal (it maximizes SIMO capacity), and produces an SNR that is the sum of the component SNRs. Note that in frequency-selective fading, this process is performed differently for each subcarrier according to its specific channel gains [23].

Transmit Diversity

The receive diversity techniques we have looked at use a single transmit and multiple receive antennas. There are also transmit-side equivalents that use multiple transmit and single receive antennas. A 2x1 setup is shown in part (b) of Figure 2.13. This can be useful when the AP has more antennas than the client, so that it can use its multiple antennas to benefit a single antenna client [23].

The transmit-side equivalent of SEL is simply to select the single best antenna on which to transmit a packet. The transmit-side equivalent of MRC is a kind of transmit beam-forming. The transmitter precodes the signals by delaying them to change the phase such that they combine constructively at the receiver's antenna, and weighting them such that transmit power is allocated to each spatial path by its SNR. These techniques are the direct analogues of the receiver-side techniques [23].

The disadvantage of transmit diversity compared to receive diversity is that the transmitter must know the channel beforehand in order to select between antennas or to precode the signals. This requires feedback from the receiver, RSSI or packet delivery statistics to inform selection and channel gains to inform precoding. Alternatively, since the properties of RF channels are reciprocal, the transmitter can learn the channel gains when it receives a packet from the target receiver. In practice, some calibration is needed to account for the differing properties of the NICs at each end. In both cases,

regular updates are needed because the channel state changes over time, often very quickly due to multi-path fading, and out of date channel gains make precoding less effective [23].

It is also worth noting that there are different beam-forming techniques that use phased antenna arrays to direct the signal. These techniques are based on precise geometric antenna arrangements (circles or lines) and orient the signal in physical space with the same pattern for each subcarrier. The precoded, measurement-based beam-forming described above has no particular physical interpretation and treats each subcarrier individually [23].

There are also an advanced class of transmit diversity techniques called space-time codes that do not need feedback to work, but instead require a change in the receiver's processing. The transmitter sends a signal coded in a particular way across antennas (space) and the data stream (time) that enables that a specialized receiver to aggregate the spatial paths. Space-time codes are simpler to use than precoding, but have worse performance for more than two transmit antennas [23].

2.3.3 Spatial multiplexing gain

MIMO systems offer a linear increase in data rate through spatial multiplexing [5, 9, 22, 35], i.e., transmitting multiple, independent data streams within the bandwidth of operation. Under suitable channel conditions, such as rich scattering in the environment, the receiver can separate the data streams. Furthermore, each data stream experiences at least the same channel quality that would be experienced by a single-input single-output system, effectively enhancing the capacity by a multiplicative factor equal to the number of streams. In general, the number of data streams that can be reliably supported by a MIMO channel equals the minimum of the number of transmit antennas and the number of receive antennas, min $\{M_T, M_R\}$. The spatial multiplexing gain increases the capacity of a wireless network [22].

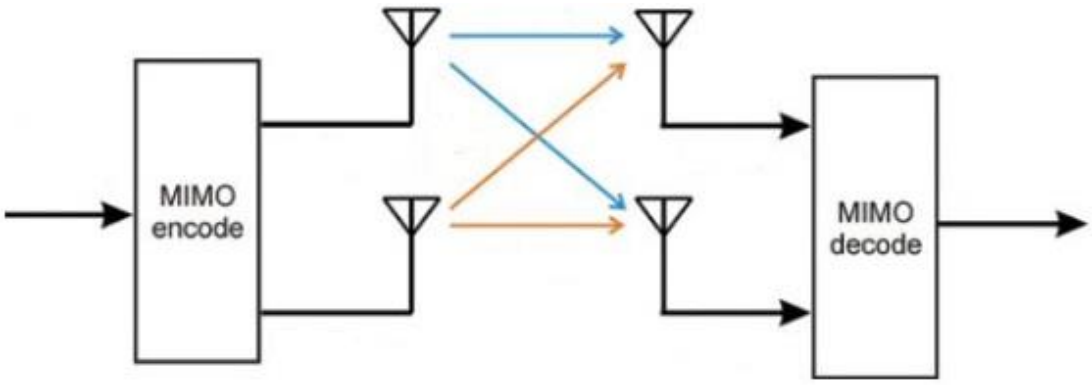

Figure 2.14 Spatial multiplexing

2.3.4 Interference reduction and avoidance

Interference in wireless networks results from multiple users sharing time and frequency resources. Interference may be mitigated in MIMO systems by exploiting the spatial dimension to increase the separation between users. For instance, in the presence of interference, array gain increases the tolerance to noise as well as the interference power, hence improving the signal-to-noise-plus-interference ratio (SINR). Additionally, the spatial dimension may be leveraged for the purposes of interference avoidance, directing signal energy towards the intended user and minimizing interference to other users. Interference reduction and avoidance improve the coverage and range of a wireless network. In general, it may not be possible to exploit simultaneously all the benefits described above due to conflicting demands on the spatial degrees of freedom. However, using some combination of the benefits across a wireless network will result in improved capacity, coverage and reliability [22].

Method	Capacity (bits/sec)
SISO	$\beta \log_2 (1+\rho)$
Diversity (1xN or Nx1)	$\beta \log_2 (1+\rho N)$
Diversity (NxN)	$\beta \log_2 (1+\rho N^2)$
Multiplexing	$\beta N \log_2 (1+\rho)$

Table 2.1 Capacity for wireless links in an ideal channel

Having multiple antennas both at the transmitter and receiver allows the use of the bigger improvement of MIMO techniques, the spatial multiplexing.

The real excitement around MIMO is that the independent paths between multiple antennas can be used to much greater effect than simply for diversity to boost the SNR. Spatial multiplexing takes advantage of the extra degrees of freedom provided by the independent spatial paths to send independent streams of information at the same time over the same frequencies. The streams will become combined as they pass across the channel, and the task at the receiver is to separate and decode them [23].

To get an idea of the potential benefits, we turn briefly to theory. For a single antenna at the transmitter and receiver, Shannon's classic formula gives the SISO capacity as shown in Table 2.1. Here, β is the system bandwidth in Hertz, and ρ is the SNR of the channel. When using diversity, N antennas using MRC (receiver) or precoding (transmitter) will achieve an N-fold increase in SNR [23].

Now consider the case where each node has N antennas and in an ideal (best-case) channel with independent spatial paths between the pairs of transmit and receive antennas. The N^2 paths provide an N^2 increase in SNR using diversity optimally. There are N spatial degrees of freedom in the system, since the signal from each transmit antenna can change the received signals in a different manner. By using the antennas to divide the transmit power over these degrees of freedom, the transmitter can divide its power to send N spatial streams of data, each getting an SNR of ρ when combined at the receiver. This is a rough argument for the theoretical capacity (Table 2.1) for a multiplexing MIMO system [24] [23].

In practice, real channels may achieve sub-linear gains in capacity using multiplexing due to spatial correlation which causes fewer than N degrees of freedom or less than perfect combining of the spatial streams of SNR ρ/N. Still, for good MIMO links at high SNR, the capacity scales nearly linearly with the number of antennas, even for a small number of antennas. That is a much larger performance improvement than adding SNR using diversity. At low SNR, however, the gain from receive antennas is the larger effect, with extra transmit antennas making little difference.

There are many ways to process signals at the transmitter and receiver to realize MIMO gains that have different trade-offs.

3. A review of IA and iterative Equalization Techniques

This chapter focuses on introducing the concepts of Interference Alignment and Iterative Equalization that will be used in chapter 4. IA is a technique that allows the coexistence of multiple signals in the same space/frequency/time in a way that can be recovered by its intended receiver. Iterative Equalization is used to further improve the linear equalizer, namely for single carrier based systems like SC-FDMA.

3.1 Interference Alignment Concept

In the absence of precise capacity characterizations, researchers have pursued asymptotic and/or approximate capacity characterizations. Capacity characterizations have been found for centralized networks (Gaussian multiple access and broadcast networks with multiple antennas), but capacity characterizations for most distributed communication scenarios remain long standing open problems [25].

It can be argued that the most preliminary form of capacity characterization for a network is to characterize its degrees of freedom (DoF). The degrees of freedom represent the rate of growth of the network capacity with the log of the signal to noise ratio (SNR). In most cases, the spatial degrees of freedom turn out to be the number of non-interfering paths that can be created in a wireless network through signal processing at the transmitters and receivers. While time, frequency and space all offer degrees of freedom in the form of orthogonal dimensions over which communication can take place, spatial degrees of freedom are especially interesting in a distributed network [25].

Recent work on degrees of freedom characterization for interference networks led to the emergence of a new concept called interference alignment (IA), which has challenged the conventional throughput limits of both wired and wireless networks. This new concept has pointed out some of the earlier work incorrect inferences such as:

1. The number of degrees of freedom for a wireless network with perfect channel knowledge at all nodes is an integer.
2. The degrees of freedom of a wireless network with a finite number of nodes are not higher than the maximum number of co-located antennas at any node.

Interference alignment allows many interfering users to communicate simultaneously over a limited number of signalling dimensions (bandwidth) by confining the interference at each receiver into a space spanned by a small number of dimensions, while keeping the desired signals separable from interference. This enables the desired signals to be projected into the null space of the interference and thereby can be recovered free from interference. Interestingly, interference alignment does for wireless networks what MIMO technology has done for the point to point wireless channel. In both cases the capacity, originally limited to log(1+SNR), is shown to be capable of linearly increasing with the number of antennas. While MIMO technology requires nodes equipped with multiple antennas, interference alignment works with the distributed antennas naturally available in a network across the interfering transmitters and receivers. For example, in the *K*-user wireless interference channel, interference alignment allows each user to simultaneously send at a data rate equal to half of his interference-free channel capacity to his desired receiver, even though the number of users *K* can be arbitrarily large. Simply put, interference alignment suggests that interference channels are not fundamentally interference limited [25].

The X network is a communication network, which consists of *Mt* transmitters and *Mr* receivers. There is a message to be sent from each transmitter to each receiver, thus constituting *MtMr* independent messages that need to be sent from all transmitters to all receivers. The Multiple access channel (MAC), the broadcast channel (BC), and the interference channel (IC) are all special cases of X networks. Thus, any outer bound on the degrees of freedom region of an X network is also an outer bound on the degrees of freedom of all its sub-networks. A general outer bound on the degrees of freedom region of an *Mt* x *Mr* wireless X network when using interference alignment is derived in [26]. Three different scenarios are discussed in; the case when all nodes are equipped with single

antennas, the case where either $Mt = 2$ or $Mr = 2$, and a scrap on the case where all nodes are equipped with A antennas. In all cases, channel coefficients are assumed to be time varying or frequency selective and drawn from a continuous distribution [25].

In Figure 3.1, an example of a 2 x 2 user X network is shown where a 4/3 degrees of freedom are shown to be achievable using interference alignment over 3 signalling dimensions, 3 antennas per user. In this example, both users are allowed to transmit two data where $\mathbf{x}_{ij}$ represents the transmitted data stream from transmitter j intended to receiver i, $\mathbf{V}_{ij}$ represent the precoding vectors at transmitter j, and $\mathbf{H}_{ij}$ represents the channel coefficients between transmitter j and receiver i [25].

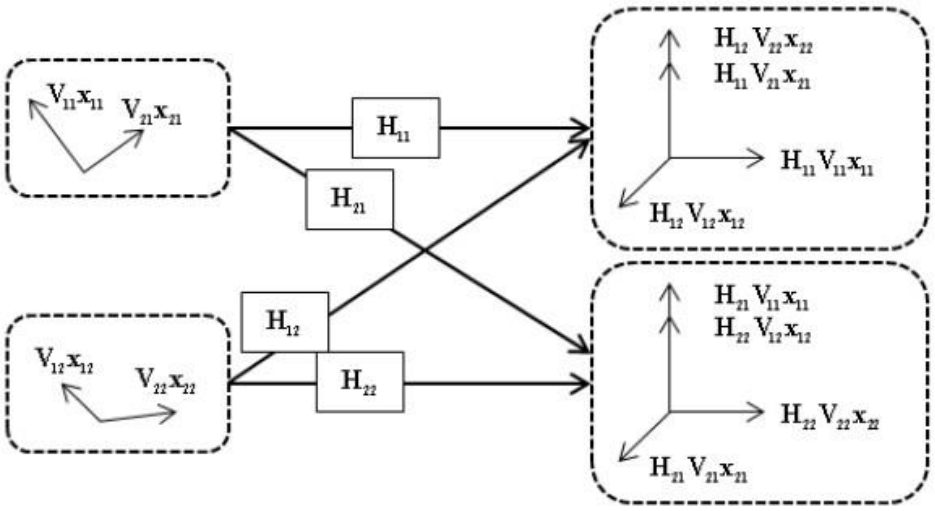

Figure 3.1 An example 2x2 user X network channel

3.1.1 Wireless X Network with Single-Antenna Nodes

An asymptotic interference alignment scheme is proposed in [26], where the total number of degrees of freedom achieved is shown to be close to $\frac{MtMr}{Mt + Mr - 1}$ with a capacity characterization within for single-antenna nodes and using large channel extensions. Another useful result is that when the number of transmitters is much larger than the number of receivers or vice versa, the Mt x Mr X network achieves a number of degrees of freedoms that is close to that achieved by an Mt x Mr MIMO network. This is evident when $Mt >> Mr$ or $Mr >> Mt$, as $\frac{MtMr}{Mt + Mr - 1}$ becomes very close to min (Mt, Mr) [25].

3.1.2 Wireless X Network with Multiple-Antenna Nodes

It is also shown in [26] that for an *Mt* x *Mr* X network where each node is equipped with *A* antennas, the total number of degrees of freedom is outer bounded by $\frac{AMtMr}{Mt+Mr-1}$ per orthogonal time and frequency dimension [25].

Moreover, a lower bound of $\frac{AMtMr}{Mt+Mr-1/A}$ is shown to be achievable in [26]. This lower bound is close to the outer bound if either *Mt* or *Mr* is reasonably large [25].

In [27], a study on the case of the 2-user X network where each node is equipped with three antennas is conducted. Three different precoding schemes based on iterative random search approach are considered in this paper. The three schemes are designed based on zero-forcing (ZF), minimum mean square error (MMSE), and maximum signal-to-leakage ratio (SLR) criteria. The proposed schemes are designed to satisfy the interference alignment conditions and at the same time optimize system performance. Three optimization approaches are considered; for ZF criteria, the optimization objective is to maximize the minimum of SINRs for each data stream, for MMSE criteria, the optimization objective is to minimize the mean square error (MSE) of the detected data, and for SLR criteria, the precoding vectors are optimized based on maximization of SLR, and the receive steering vectors are optimized based on maximization of SINR. Simulation results show that the proposed schemes are very efficient and can provide good performance for the MIMO network [25].

3.2 Iterative Equalization

Linear equalizers offer a reasonable complexity/performance commitment, however they have several problems, namely noise enhancement and residual ISI (Inter-Symbol Interference). Non-linear have better performance than using the linear approach. DFE is a popular choice since it provides a good trade-off between complexity and performance. Its basic structure is depicted in figure 3.2 [28].

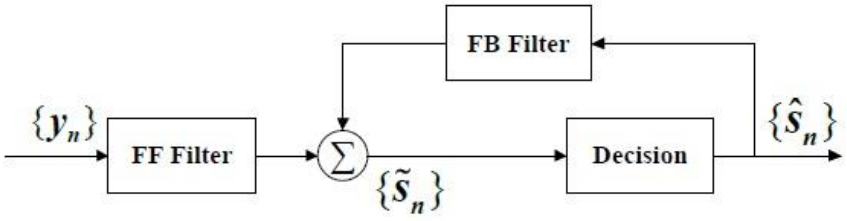

Figure 3.2 Basic DFE structure

A nonlinear equalizer with a DFE component is simply implementing a feedback filter (FB Filter) to the output of the feedforward block samples (derived from the FF filter), and making this process into an iterative scheme, makes the DFE an efficient equalizer for the received signals. The linear DFE is replaced by an Iterative-Block Decision Feedback Equalization (IB-DFE) [29], which corresponds to an iterative DFE for SC-FDA where the feedforward and feedback operations are implemented in the frequency domain as shown in picture 3.3 [28].

In this section, capital letters denote frequency domain and lower letters the time domain.

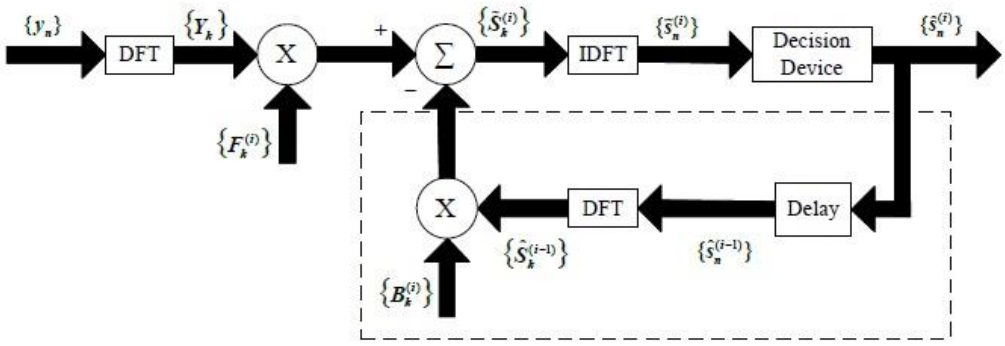

Figure 3.3 Basic IB-DFE block diagram for single user

Using IB-DFE and regarding the i^{th} iteration, the frequency domain block can be characterized as

$$\tilde{S}_k^{(i)} = F_k^{(i)} Y_k - B_k^{(i)} \hat{S}_k^{(i-1)} \tag{3.1}$$

where $\left\{\tilde{S}_k^{(i)}; k = 0,1,\ldots,N-1\right\}$ is the output of the equalizer, $\left\{F_k^{(i)}; k = 0,1,\ldots,N-1\right\}$ is the feedforward coefficient and $\left\{B_k^{(i)}; k = 0,1,\ldots,N-1\right\}$ is the feedback coefficient from the DFE block. $\left\{\hat{S}_k^{(i-1)}; k = 0,1,\ldots,N-1\right\}$ is the DFT of the "hard decision" block $\left\{\hat{s}_n^{(i-1)}; k = 0,1,\ldots,N-1\right\}$ from the previous iteration related with the transmitted domain block $\left\{s_n; n = 0,1,\ldots,N-1.\right\}$ [28].

The feedforward and feedback coefficients are chosen in order to maximize the SINR (Signal to Interference plus Noise Ratio) and in an IB-DFE receiver are given by

$$F_k^{(i)} = \frac{H_k^*}{SNR + \left(1 - \left(\rho^{(i-1)}\right)^2\right)\left|H_k\right|^2} \tag{3.2}$$

and

$$B_k^{(i)} = \rho^{(i-1)} \left(F_k^{(i)} H_k - 1 \right) \tag{3.3}$$

The ρ factor corresponds to the correlation coefficient and is defined as

$$\rho^{(i-1)} = \frac{\mathbb{E}\left[\hat{S}_k^{(i-1)} S_k^* \right]}{\mathbb{E}\left[\left| S_k \right|^2 \right]} = \frac{\mathbb{E}\left[\hat{s}_n^{(i-1)} s_n^* \right]}{\mathbb{E}\left[\left| s_n \right|^2 \right]} \tag{3.4}$$

The block $\left\{ \hat{s}_n^{(i-1)}; n = 0, 1, \ldots, N-1 \right\}$ denotes the data estimates associated to the previous iteration. The correlation coefficient is a crucial parameter to ensure a good receiver performance, given that it supplies a block-wise reliability measure of the estimates employed in the feedback loop. This is done in the feedback loop by taking into account the hard decisions for each block plus the overall block reliability, which reduces error propagation problems [28].

With a conventional IB-DFE receiver the log-likelihood values are computed on a symbol-by-symbol basis (no need to perform the channel decoding in the feedback loop). Therefore, conventional IB-DFE receivers can be considered as low complexity turbo equalizers when the feedback loop employs the equalizer outputs rather than the channel decoder outputs. For the first iteration $(i = 0)$, no information exists about $\mathbf{s}_n$, meaning that $\rho = 0$, $B_k^{(0)} = 0$ and $F_k^{(0)}$ corresponds to the expression of a normal MMSE (the IB-DFE receiver is reduced to a linear FDE for the first iteration). After the first iteration the feedback coefficients can be applied to reduce a major part of the residual interference, and after several iterations and for a moderate-to-high SNR, the correlation coefficient tends to be $\rho \approx 1$ and the residual ISI will be almost totally cancelled [28].

Figure 3.4 shows the BER performance evolution for a transmission system with SC uncoded modulation that uses an IB-DFE receiver with 4 iterations total, and for the sake of comparison the performance of the MFB is also presented. From the results, it can be seen that the Eb / N_0 required for BER=10^{-4}, for the first iteration (that corresponds to the linear SC-FDE), is approximately 15.5 dB, descending to 11 dB after only three iterations, being clear that the use of the iterative receiver allows a significate performance improvement. Also, the asymptotic BER performance becomes close to the MFB after a few iterations, since the computation of the correlation coefficient becomes more reliable, as a consequence of the information from the previous iteration(s). Hence, the estimated samples become close to the transmitted ones [28].

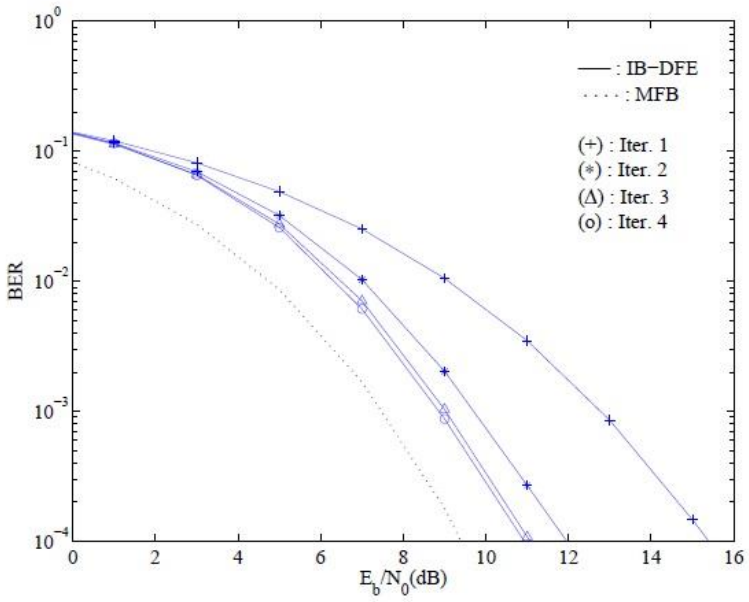

Figure 3.4 BER performance for an IB-DFE receiver

3.2.1 IB-DFE with Hard Decisions

The focus is now going to be in hard decisions of the estimated samples, in the IB-DFE process, wherein the decision is made at a block level [28].

In order to calculate the receiver parameters, it was assumed that the global channel frequency response is

$$F_k^{(i)} H_k \tag{3.5}$$

The residual ISI component, in the frequency-domain is related with the difference between the global channel frequency response given by (3.5) and

$$\gamma^{(i)} = \frac{1}{N} \sum_{k=0}^{N-1} F_{\mathrm{k}}^{(\mathrm{i})} H_{\mathrm{k}} \tag{3.6}$$

We can regard $\gamma^{(\mathrm{i})}$ as the average overall channel frequency response at the i^{th} iteration. Nevertheless, if the estimates of the transmitted block are reliable, the feedback filter can be employed

to eliminate the residual ISI. The equalized samples related to each iteration, in the frequency-domain, are then given by

$$\tilde{S}_k^{(i)} = \gamma^{(i)} S_k + \varepsilon_k^{(i)} \tag{3.7}$$

where $\varepsilon_k^{(i)}$ represents the global error consisting of the residual ISI plus the channel noise. As previously mentioned, the feedforward and feedback IB-DFE coefficients are chosen in order to maximize the SINR, as

$$SINR = \frac{\left|\gamma^{(i)}\right|^2 \mathbb{E}\left[\left|S_k\right|^2\right]}{\mathbb{E}\left[\left|\varepsilon_k^{(i)}\right|^2\right]} \tag{3.8}$$

The DFE estimated frequency-domain data samples $\hat{S}_k^{(i)}$ can be expressed as

$$\hat{S}_k^{(i)} = \rho^{(i)} S_k + \Delta_k^{(i)} \tag{3.9}$$

where ρ is similar to the one denoted in (3.4) and $\Delta_k^{(i)}$ denotes a zero-mean error term for the k^{th} frequency-domain hard decision estimate. Assuming $\mathbb{E}\left[\Delta_k^{(i)}\right] = 0$ and $\mathbb{E}\left[\Delta_k^{(i)} S_{k'}^{(i)*}\right] \approx 0$ for $k' \neq k$ then

$$\mathbb{E}\left[\left|\Delta_k^{(i)}\right|^2\right] \approx \left(1 - \left(\rho^{(i)}\right)^2\right) \mathbb{E}\left[\left|S_k\right|^2\right] \tag{3.10}$$

Combining the expression for a received signal

$$Y_k = H_k S_k + N_k \tag{3.11}$$

with (3.1) and (3.9) it can be written that

$$\tilde{S}_k^{(i)} = \gamma^{(i)} S_k + \left(F_k^{(i)} H_k - \gamma^{(i)} - \rho^{(i-1)} B_k^{(i)} \right) S_k - B_k^{(i)} \Delta_k^{(i-1)} + F_k^{(i)} N_k \quad (3.12)$$

It can be concluded that $\tilde{S}_k^{(i)}$ has the following components

- The first term, $\gamma^{(i)} S_k$, denotes the useful signal component.
- The second term, $\left(F_k^{(i)} H_k - \gamma^{(i)} - \rho^{(i-1)} B_k^{(i)} \right) S_k$, refers to the residual ISI factor.
- The third term, $B_k^{(i)} \Delta_k^{(i-1)}$, denotes the noise originated by feedback errors (errors in the decision estimates $\hat{s}_n^{(i-1)}$ that are reintroduced in the system)
- The fourth term, $F_k^{(i)} N_k$, denotes the channel noise.

Finally $\tilde{S}_k^{(i)}$ can be written as

$$\tilde{S}_k^{(i)} = \gamma^{(i)} S_k + E_k \quad (3.13)$$

with denoting the overall error for the k^{th} frequency-domain symbol, that is given by

$$E_k = \left(F_k^{(i)} H_k - \gamma^{(i)} - \rho^{(i-1)} B_k^{(i)} \right) S_k - B_k^{(i)} \Delta_k^{(i-1)} + F_k^{(i)} N_k \quad (3.14)$$

From [30], the maximization of the SINR results in the optimum values of the feedforward and feedback coefficients given by

$$F_k^{(i)} = \frac{SNR\left(1 - \left(\rho^{(i-1)}\right)^2\right)\gamma^{(i)} H_k^*}{1 + SNR\left(1 - \left(\rho^{(i-1)}\right)^2\right)\left|H_k\right|^2} \quad (3.15)$$

and

$$B_k^{(i)} = \rho^{(i-1)} \left(F_k^{(i)} H_{\mathrm{k}} - \gamma^{(i)} \right) \tag{3.16}$$

with $SNR = \frac{E_s}{2\sigma_N^2}$ and with $E_s = \mathbb{E}\left[\left| s_n \right|^2 \right]$ denoting the average symbol energy. Multiplying all the $F_{\mathrm{k}}^{(\mathrm{i})}$ coefficients by a constant does not alter the SINR, therefore (3.15) can be written as

$$F_{\mathrm{k}}^{(\mathrm{i})} = \frac{\xi^{(i)} H_k^*}{NSR + \left(1 - \left(\rho^{(i-1)} \right)^2 \right) \left| H_{\mathrm{k}} \right|^2} \tag{3.17}$$

where $\zeta^{(i)}$ is selected to ensure that $\gamma^{(i)} = 1$ [28].

3.2.2 IB-DFE with Soft Decisions

The performance driven from the Iterative-Block Decision Feedback Equalization (IB-DFE) receiver can be improved, by considering "soft decisions" instead of "hard decisions", which means that the "blockwise average" is substituted by "symbol averages". Hence, the samples $\hat{s}_n^{(i)}$ are substituted by the soft decision resulting samples $\overline{s}_n^{(i)}$ [28].

Under these assumptions the equation 3.1 can take the form

$$\tilde{S}_k^{(i)} = F_k^{(i)} Y_k - B_k^{(i)} \overline{S}_k^{(i-1)} \tag{3.18}$$

where

$$\overline{S}_k^{(i-1)} = \rho^{(i-1)} \hat{S}_k^{(i-1)} \tag{3.19}$$

Since $\rho^{(i-1)}$ is a measure of the blockwise reliability of the estimates expressed by $\hat{S}_{\boldsymbol{k}}^{(\boldsymbol{i}-1)}$, it has the consequence of $\overline{S}_{\boldsymbol{k}}^{(\boldsymbol{i}-1)}$ representing the overall block average of $S_k^{(i-1)}$ at the output of the FDE

processing. Considering a transmission system with respect to the use of a QPSK constellation (for example, under a Gray mapping rule), the symbols correspond to $s_n = \pm 1 \pm 1 = s_n^I + s_n^Q$, where $s_n^I = \mathrm{Re}\{s_n\}$ and $s_n^Q = \mathrm{Im}\{s_n\}$. Thus, the LogLikelihood Ratios (LLRs) of the in-phase bit and the quadrature bit, associated to s_n^I and s_n^Q, are given by

$$L_n^{I(i)} = \frac{2}{\sigma_i^2} \tilde{s}_n^{I(i)} \tag{3.20}$$

and

$$L_n^{Q(i)} = \frac{2}{\sigma_i^2} \tilde{s}_n^{Q(i)} \tag{3.21}$$

The conditional expectations associated with the data symbols are

$$\bar{s}_n^{(i)} = \tanh\left(\frac{L_n^{I(i)}}{2}\right) + j \tanh\left(\frac{L_n^{Q(i)}}{2}\right) = \rho_n^I \hat{s}_n^I + j \rho_n^Q \hat{s}_n^Q \tag{3.22}$$

with the signs of L_n^I and L_n^Q defining the hard decisions $\hat{s}_n^I = \pm 1$ and $\hat{s}_n^Q = \pm 1$.

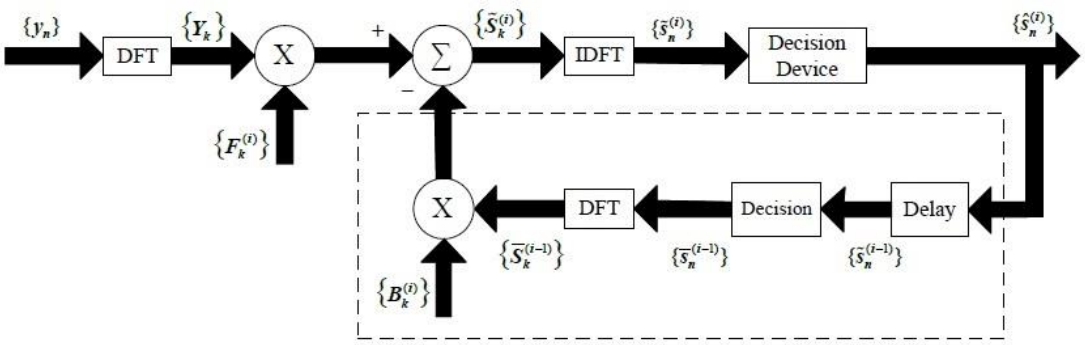

Figure 3.5 IB-DFE receiver block with soft decisions

In (3.22) ρ_n^I and ρ_n^Q denote the reliabilities related to the in-phase bit and the quadrature bit of the n^{th} symbol, are given by

$$\rho_n^{I(i)} = \left| \tanh\left(\frac{L_n^{I(i)}}{2} \right) \right| \tag{3.23}$$

$$\rho_n^{Q(i)} = \left| \tanh\left(\frac{L_n^{Q(i)}}{2} \right) \right| \tag{3.24}$$

For the first iteration $\rho_n^{I(0)} = \rho_n^{Q(0)} = 0$, and consequently $\overline{s}_n = 0$. The correlation coefficient employed in the feedforward coefficients is expressed by

$$\rho^{(i)} = \frac{1}{2N} \sum_{n=0}^{N-1} \left(\rho_n^{I(i)} + \rho_n^{Q(i)} \right) \tag{3.25}$$

The receiver structure for the IB-DFE with soft decisions, is illustrated in Figure 3.5. It can be noticed that the receiver that employs blockwise reliabilities is referred as IB-DFE with hard decisions, while the receiver that employs symbol reliabilities is referred as IB-DFE with soft decisions. The feedforward coefficients used in both types of IB-DFE receivers are given by (3.17), however the feedback loop of the IB-DFE with hard decisions uses the estimated data block, weighted by a reliability coefficient common to the entire block, while for IB-DFE with soft decisions the feedback loop uses a different reliability coefficient for each symbol [28].

4. Joint pre-coding and equalization techniques for SC-FDMA

In this Chapter we present and evaluate the proposed joint interference alignment (IA) precoding at the small cell user terminals (UTs) with iterative non-linear frequency domain equalizer at the receivers (macro base station and central unit) for SC-FDMA based heterogeneous networks. We assume that a set of small cells coexist with a macro-cell within the same spectrum, and therefore interfere to each other. Thus, to enable transmissions from the small-cells, without any performance degradation at the macro-cell, we enforce that all interference generated by the small cells is aligned in an orthogonal subspace to the macro-cell received signal space. Then, we design an iterative nonlinear frequency domain equalizer at the macro-cell receiver that is able to recover the macro-cell spatial streams, in the presence of both small-cell and inter-carrier interferences. For the small cells we consider that the access points are connected through a limited capacity backhaul network to a central unit (CU) where the separation of the small-cell signals is also performed through an iterative nonlinear frequency domain equalizer. The matrices for these two nonlinear space-frequency equalizers are obtained by minimizing the overall mean square error of all data streams at each subcarrier. The results have shown that the proposed receiver structures are robust to the inter-system interferences and are able to efficient separate the macro and small cells spatial streams.

4.1 System Model

Let us consider a scenario where a set of *N* small cells are within the coverage area of a macro-cell, sharing the same spectrum. The *N* small cells access points (AP) are all connected by a backhaul network to a central unit (CU) that provides the joint processing for the received signals. The uplink for both the macro and small-cells uses single-carrier FDMA (SC-FDMA) as the access technique, with *L* available subcarriers.

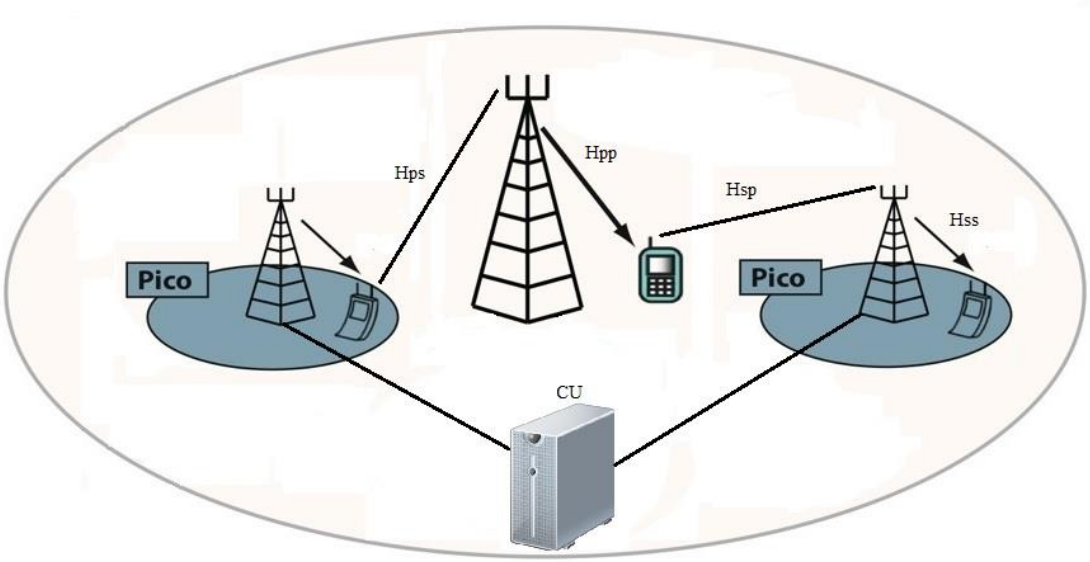

Figure 4.1 Set of small-cells within a macro-cell

- *Macro-Cell System*

The macro-cell has a BS and an associated UT. The number of antennas at the BS and UT_0 is *M* and $M_0 = M - 1$, respectively. The received frequency-domain signal (i.e., after cyclic prefix removal and FFT operation) at the macro-cell system (i.e. at the macro BS) on the *l*th subcarrier is given by:

$$\mathbf{y}_p^l = \underbrace{\mathbf{H}_{pp}^l \mathbf{x}_p^l}_{\text{Desired Signal}} + \underbrace{\mathbf{H}_{ps}^l \mathbf{x}_s^l}_{\text{Inter-System Interference}} + \underbrace{\mathbf{n}_p^l}_{\textit{Noise}} \tag{4.1}$$

where $\mathbf{H}_{pp}^l \in \mathbb{C}^{M \times M_0}$ and $\mathbf{H}_{ps}^l \in \mathbb{C}^{M \times MN}$ denote the channel between macro UT and the BS and the channels between small-cell UTs and the BS on the *l*th subcarrier, respectively. The channel matrix $\mathbf{H}_{ps}^l$ is a block matrix, i.e. $\mathbf{H}_{ps}^l = \left[\mathbf{H}_{ps,1}^l \quad \cdots \quad \mathbf{H}_{ps,N}^l\right]$, where $\mathbf{H}_{ps,N}^l$ denotes the channel matrix between UT_N and the BS. $\mathbf{x}_p^l \in \mathbb{C}^{M_0 \times 1}$ represents the macro-cell UT_0 transmit signal on the *l*th subcarrier, $\mathbf{x}_s^l =$

$\left[\mathbf{x}_{s,1}^H \quad \cdots \quad \mathbf{x}_{s,n}^H \quad \cdots \quad \mathbf{x}_{s,N}^H\right]^H \in \mathbb{C}^{MN\times 1}$ the concatenation of all small-cell UT transmit signals on the *l*th subcarrier and $\mathbf{n}_p^l$ white Gaussian noise with variance σ_{noise}^2.

The macro UT uses all available spatial resources for data transmission, i.e., M_0 data streams are transmitted at each subcarrier. Let us denote by $\mathbf{d}_p^l \in \mathbb{C}^{M_0\times 1}$ the vector of data symbols transmitted at subcarrier *l* and by $\mathbf{d}_p^l(j)$ the corresponding *j* element (with $\mathbb{E}[|\mathbf{d}_p^l(j)|^2] = P_p$). The data symbols are drawn from an *M*-QAM constellation. To form the transmit signal, the macro UT applies a discrete Fourier transform (DFT) to the sequence $\{\mathbf{d}_p^l(j)\}_{l=1}^L$

$$\{\mathbf{x}_p^l(j)\}_{l=1}^L = \mathrm{DFT}(\{\mathbf{d}_p^l(j)\}_{l=1}^L) \tag{4.2}$$

- *Small-Cells*

It is considered that each small-cell has one access point (AP) and an associated UT. It is assumed that each AP and each UT is equipped with M antennas. The received signal $\mathbf{y}_s^l \in \mathbb{C}^{MN\times 1}$ in frequency domain at the central unit of all APs and subcarrier *l* is

$$\mathbf{y}_s^l = \underbrace{\mathbf{H}_{ss}^l \mathbf{x}_s^l}_{\text{Desired Signal}} + \underbrace{\mathbf{H}_{sp}^l \mathbf{x}_p^l}_{\substack{\text{Inter-System}\\ \text{Interference}}} + \underbrace{\mathbf{n}_s^l}_{\text{Noise}}, \tag{4.3}$$

where $\mathbf{H}_{ss}^l \in \mathbb{C}^{MN\times MN}$ and $\mathbf{H}_{sp}^l \in \mathbb{C}^{MN\times M_0}$ denote the overall channels between the small-cell UTs to the APs and channel between the macro-cell UT_0 to the APs on the *l*th subcarrier, respectively. The matrix $\mathbf{H}_{ss}^l = \left[\mathbf{H}_{ss,1}^l \quad \cdots \quad \mathbf{H}_{ss,n}^l \quad \cdots \quad \mathbf{H}_{ss,N}^l\right]$, where $\mathbf{H}_{ss,n}^l = \left[\mathbf{H}_{ss,n,1}^{lH} \quad \cdots \quad \mathbf{H}_{ss,n,i}^{lH} \quad \cdots \quad \mathbf{H}_{ss,n,N}^{lH}\right]$ and $\mathbf{H}_{ss,n,i}^{lH}$ represents the channel matrix between the *n*th small-cell UT and the *i*th AP. $\mathbf{n}_s^l$ is zero mean white Gaussian noise with variance σ_{noise}^2. The transmit signal at small-cell UT *n* is obtained through the linear map $\mathbf{v}_{s,n}^l$

$$\mathbf{x}_{s,n}^l = \mathbf{v}_{s,n}^l z_{s,n}^l, \tag{4.4}$$

The sequence $\{z_{s,n}^l\}_{l=1}^L$ is the DFT of the data symbols $\{d_{s,n}^l\}_{l=1}^L$, $n = \{0,1,\ldots,N\}$, with $\mathbb{E}[|d_{s,n}^l|^2] = P_s$ and the data symbols are drawn from a *M*-QAM constellation. Note that for the small-cells we apply a

precoder, in frequency domain, to the sequence $\{z_{s,n}^l\}_{l=1}^L$ before transmission. The precoder $\mathbf{v}_{s,n}^l \in \mathbb{C}^{M\times 1},\ \forall n \in \{1,\ldots,N\}$ is unitary, i.e. $(\mathbf{v}_{s,n}^l)^H \mathbf{v}_{s,n}^l = 1$

4.2 Precoders/Equalizers Design

In this section, we design the precoders employed at the small-cell UTs to align all the generated interference at the macro-cell BS. We also derive new iterative frequency domain equalizers for both the macro and small-cells such that they can coexist under the same spectrum.

- Precoders design

From equation (4.1) we verify that, at the *l*th subcarrier, the macro-cell signal spans the column space of matrix $\mathbf{H}_{pp}^l$. Therefore, to enable transmissions from the small-cells without any performance degradation at the macro-cell we must enforce that all interference must be contained in an orthogonal subspace to the signal space. Let us denote by $\mathbf{a}_s^l \in \mathbb{C}^M$ the interference subspace, then the UT *n* precoder can be mathematically described by

$$\mathbf{v}_{s,n}^l = \gamma_n^l (\mathbf{H}_{ps,n}^l)^{-1} \mathbf{a}_s^l \tag{4.5}$$

where $\gamma_n^2 = P_s / (\mathbf{a}_s^{l^H} (\mathbf{H}_{ps,n}^l \mathbf{H}_{ps,n}^{l^H})^{-1} \mathbf{a}_s^l)$ is a normalizing constant to settle the power of the transmit signal of UT *n* to P_s.

In the following we assume that the BS broadcasts alignment vector $\mathbf{a}_s^l$, through a dedicated channel or the existing backhaul infrastructure, to the small-cells, which after the reception of this information design their precoders according to (4.7). It can be easily verified from equation (4.1) and (4.5) that the received signal at the BS is now given by

$$\mathbf{y}_p^l = \underbrace{\mathbf{H}_{pp}^l \mathbf{x}_p^l}_{\text{Desired Signal}} + \underbrace{\left(\sum_{n=1}^{N} \gamma_n^l z_{s,n}^l\right) \mathbf{a}_s^l}_{\text{Inter-System Interference}} + \underbrace{\mathbf{n}_p^l}_{\text{Noise}} \tag{4.6}$$

To make the signal and interference subspaces orthogonal, as mentioned before, we must have

$$\mathbf{a}_s^l = \mathcal{N}(\mathbf{H}_{pp}^l) \tag{4.7}$$

The interference subspace may be obtained by applying the singular value decomposition (SVD) to the macro channel, as the null space of the macro-channel, is given by the left singular vector

associated with the zero singular value. As the BS has M antennas and needs $M_0 = M - 1$ dimensions to resolve the transmitted signal, then only one dimension is left for small cell transmission. By using IA, this free space dimension can be reutilized by all small-cells to transmit one stream each.

- *Iterative equalizer design for the macro-cell*

It is well known that for SC-FDMA based systems, linear equalization is not efficient to separate the spatial streams due to the residual inter-carrier interference. In the context, of heterogeneous systems the equalizer should be designed to deal with both IC and inter-system interferences. Therefore, a conventional linear equalizer design may not be the best strategy.

In this section, we design an iterative nonlinear space-frequency domain equalizer based on IB-DFE principles to tackle at the same time the inter-system and IC interferences.

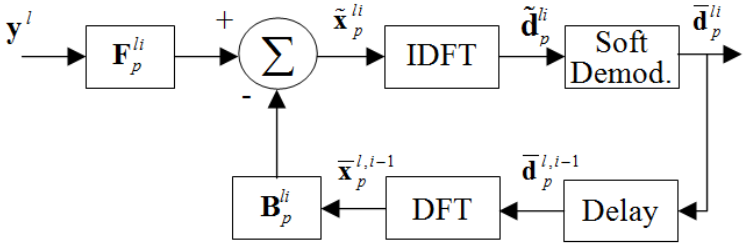

Figure 4.2 Iterative macro-cell receiver structure based on IB-DFE principle

A block diagram of the proposed IB-DFE receiver structure is depicted in figure 4.2. At the *i*th iteration, the received signal on the *l*th subcarrier, before the IDFT operation is given by

$$\tilde{\mathbf{x}}_p^{li} = \mathbf{F}_p^{li}\mathbf{y}_p^l - \mathbf{B}_p^{li}\bar{\mathbf{x}}_p^{l,i-1} \tag{4.8}$$

where $\bar{\mathbf{x}}_p^{li} = [\bar{\mathbf{x}}_p^{li}(1),\ldots,\bar{\mathbf{x}}_p^{li}(j),\ldots,\bar{\mathbf{x}}_p^{li}(M_0)]^T$. $\mathbf{F}_p^{li} \in \mathbb{C}^{M_0 \times M}$ denotes the feedforward matrix and $\mathbf{B}_p^{li} \in \mathbb{C}^{M_0 \times M_0}$ the feedback matrix. The L- length sequence $\{\bar{\mathbf{x}}_p^{li}(p)\}_{l=1}^L$ is the IDFT of the detector output $\{\bar{\mathbf{d}}_p^{li}(j)\}_{l=1}^L$. It can be shown that $\bar{\mathbf{x}}_p^{l,i} \approx \mathbf{\Psi}_p^{i^2}\bar{\mathbf{x}}_p^l + \mathbf{\Psi}_p^i\mathbf{e}_p^l$, where $\mathbf{e}_p^l$ is a zero mean error vector and $\mathbf{\Psi}_p^i$ is a diagonal correlation matrix, where the correlation coefficient computed for the jth L-length data block is

$$\boldsymbol{\Psi}_p^i(j) = \frac{\mathbb{E}\left[\hat{\mathbf{d}}_p^{l,i-1}(j)\mathbf{d}_p^{l^*}(j)\right]}{\mathbb{E}\left[\left|\mathbf{d}_p^l(j)\right|^2\right]}, \quad l = 1,\ldots,L \tag{4.9}$$

This scalar $\boldsymbol{\Psi}_p^i(j)$ represents a measure of the reliability of the estimates of the *j*th *L*-length data block associated to the *i*th iteration. For QPSK $\boldsymbol{\Psi}_p^i(j)$ can be obtained as described in [31], and for larger constellations as described in [32]. For the sake of simplicity and without loss of generality in this work we consider only QPSK constellations. Therefore, the hard decision $\hat{\mathbf{d}}_p^{li}(j)$ associated to data symbol $\hat{\mathbf{d}}_p^l(j)$ is

$$\hat{\mathbf{d}}_p^{li}(j) = \text{sign}\left(\text{Re}\left\{\tilde{\mathbf{d}}_p^{li}(j)\right\}\right) + \text{sign}\left(\text{Im}\left\{\tilde{\mathbf{d}}_p^{li}(j)\right\}\right) \tag{4.10}$$

For a given iteration, we have seen that the iterative non-linear equalizer is characterized by the matrices $\mathbf{F}_p^{li}$ and $\mathbf{B}_p^{li}$, which are selected to minimize the overall $\text{MSE}_l = \mathbb{E}\left[\left\|\tilde{\mathbf{x}}_p^l - \mathbf{x}_p^l\right\|^2\right]$ at each subcarrier. Thus the optimization problem is the following

$$\min_{\mathbf{F}_p^l, \mathbf{B}_p^l} \text{MSE}_l \text{ s.t } \frac{1}{L}\sum_{l=1}^{L} \text{tr}\left(\mathbf{F}_p^l \mathbf{H}_{pp}^l\right) = M_0 \tag{4.11}$$

By applying the Karush–Kuhn–Tucker (KKT) conditions to optimization problem we obtain the solutions

$$\mathbf{F}_p^{li} = \boldsymbol{\Omega}_p^i \mathbf{H}_{pp}^{l^H} (\mathbf{A}_p^l)^{-1} \tag{4.12}$$

$$\mathbf{B}_p^{li} = \mathbf{F}_p^{li} \mathbf{H}_{pp}^l - \mathbf{I}_{M_0}, \tag{4.13}$$

$$\boldsymbol{\Omega}_p^i = \left(\mathbf{I}_{M_0} - \boldsymbol{\Psi}_p^{(i-1)^2}\right) - \frac{\mu_p}{P_p L}\mathbf{I}_{M_0}. \tag{4.14}$$

where $\mathbf{A}_p^l = \mathbf{H}_{pp}^l(\mathbf{I}_{M_0} - \mathbf{\Psi}_p^{(i-1)^2})\mathbf{H}_{pp}^{l^H} + N\mathbf{a}_s^l\mathbf{a}_s^{l^H} + \frac{\sigma_{noise}^2}{P_p}\mathbf{I}_M$ and μ_p is the Lagrangian multiplier. The Lagrangian multiplier is selected, at each iteration i, to ensure that the constraint $\sum_{l=1}^{L} \mathrm{tr}(\mathbf{F}_p^l\mathbf{H}_{\mathrm{pp}}^l) = LM_0$ is fulfilled. For the first iteration $(i=1)$ matrix $\mathbf{\Psi}_p^0$ and vector $\bar{\mathbf{x}}_p^{l,0}$ are respectively, a null matrix and a null vector.

- *Iterative equalizer design for the small-cells*

At the CU we use the same principle to separate the small-cell UTs streams. Now, from (4.3) we verify that the interference signal subspace, at subcarrier *l*, is completely defined by matrix $\mathbf{H}_{sp}^l$. Therefore the $\mathrm{MSE}_l = \mathbb{E}[\| \tilde{\mathbf{z}}_s^l - \mathbf{z}_s^l \|^2]$ optimization problem for the small-cells is

$$\min_{\mathbf{F}_s^l, \mathbf{B}_s^l} \mathrm{MSE}_l \ \text{s.t} \ \frac{1}{L}\sum_{l=1}^{L} \mathrm{tr}\left(\mathbf{F}_s^l\mathbf{H}_{ss,eq}^l\right) = N \tag{4.15}$$

where $\tilde{\mathbf{z}}_s^{l^H} = [\tilde{z}_{s,1}^{l^H}, \ldots, \tilde{z}_{s,N}^{l^H}]^H$ denote the frequency domain samples and $\mathbf{H}_{ss,eq}^l = [\mathbf{H}_{ss,1}^l\mathbf{v}_{s,1}^l, \ldots, \mathbf{H}_{ss,N}^l\mathbf{v}_{s,N}^l]$ denote the small cell equivalent channel (both channel and precoder included).By using the Lagrangian and KKT conditions associated to optimization problem we obtain the solution, for the CU IB-DFE equalizer

$$\mathbf{F}_s^{li} = \mathbf{\Omega}_s^i\mathbf{H}_{ss,eq}^{l^H}(\mathbf{A}_s^l)^{-1} \tag{4.16}$$

$$\mathbf{B}_s^{li} = \mathbf{F}_s^{li}\mathbf{H}_{ss,eq}^l - \mathbf{I}_N, \tag{4.17}$$

$$\mathbf{\Omega}_s^i = \left(\mathbf{I}_N - \mathbf{\Psi}_s^{(i-1)^2}\right) - \frac{\mu_s}{P_s L}\mathbf{I}_N. \tag{4.18}$$

where $\mathbf{A}_s^l = \mathbf{H}_{ss,eq}^l\left(\mathbf{I}_N - \mathbf{\Psi}_s^{(i-1)^2}\right)\mathbf{H}_{ss,eq}^{l^H} + \mathbf{H}_{sp}^l\mathbf{H}_{sp}^{l^H} + \frac{\sigma_{noise}^2}{P_s}\mathbf{I}_M$. $\mathbf{\Psi}_s^i$ represents a measure of the reliability of the estimates of the *j*th *L*-length data block associated to the *i*th iteration, for the small-cell.

4.3 PERFORMANCE RESULTS

In this section we present a set of performance results for the proposed joint IA-precoding with IB-DFE based receiver structures. Most of these results have been published in an international conference.

Two different scenarios are considered:

- Scenario 1, we assume the macro-cell UT is equipped with single antenna ($M_0 = 1$), both the macro-BS, secondary UT's and small-cell access points have 2 antennas ($M = 2$).
-
- Scenario 2, we assume the macro-cell UT is equipped with two antennas ($M_0 = 2$), both the macro-BS, secondary UT's and small-cell access points have 3 antennas ($M = 3$).

In both scenarios the number of small-cells was set to 2 ($N = 2$). In the first configuration, the macro-cell UT may transmit a single data stream per sub-carrier and for the second they can transmit 2 streams per sub-carrier. For both cases each small-cell UTs transmit a single data stream per sub-carrier. The block size is $L = 128$ as well as FFT size and a QPSK constellation with Gray mapping was adopted. The channels between each transmitter and receiver pair are uncorrelated and severely time-dispersive, each one with rich multipath propagation and uncorrelated Rayleigh fading for different multipath components. Specifically, we assume L_p =32, equal power multipath components with uncorrelated Rayleigh fading. The same conclusions could be drawn for other multipath fading channels, provided that the number of separable multipath components is high. In addition, we assume perfect channel state information and synchronization. Our performance results are presented in terms of the average bit error rate (BER) as a function of E_b / N_0, with E_b denoting the average bit energy and N_0 denoting the one-sided noise power spectral density. For the sake of comparisons we include the matched filter bound (MFB).

Let's start by considering the scenario 1. In Figure 4.3 and Figure 4.4 we present results for the macro-cell and small-cells, i.e. at the BS and CU, respectively. For both we present results for the first, second and forth iterations of the proposed receiver. As expected, the BER performance improves with the iterations and its can be observed that for 2-4 iterations the performance is close the one obtained by the MFB. This means that our schemes are quite efficient to remove both the ICI and inter-systems interference allowing an effective coexistence of both systems.

Note that for the first iteration the proposed non-linear equalizers reduce to the linear MMSE based equalizer.

- *Graphical results for scenario 1*

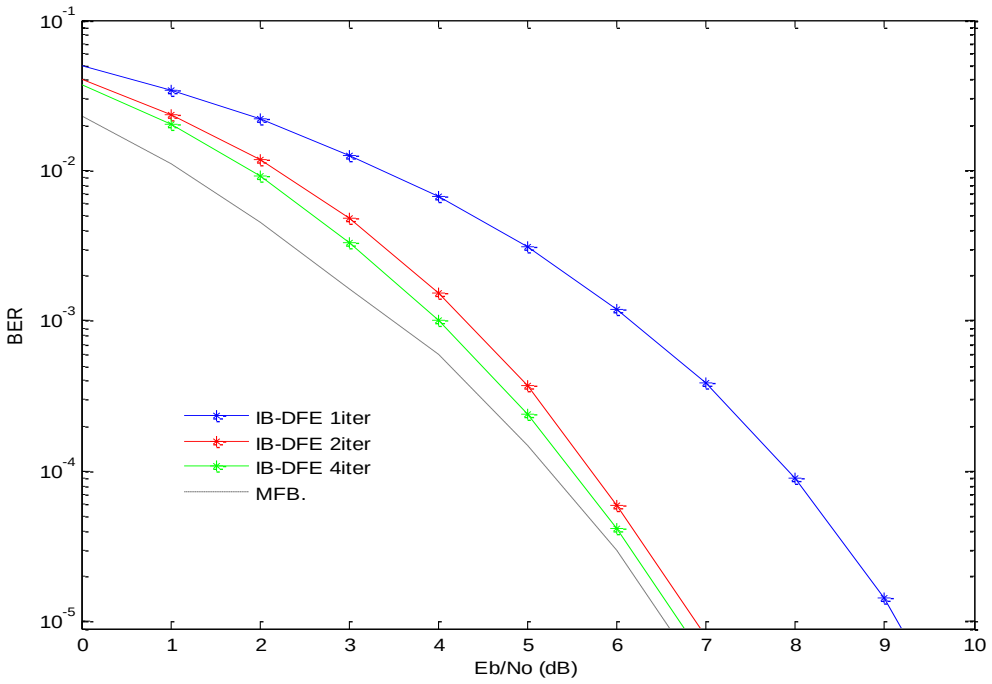

Figure 4.3 Performance evaluation at the macro-cell for scenario 1

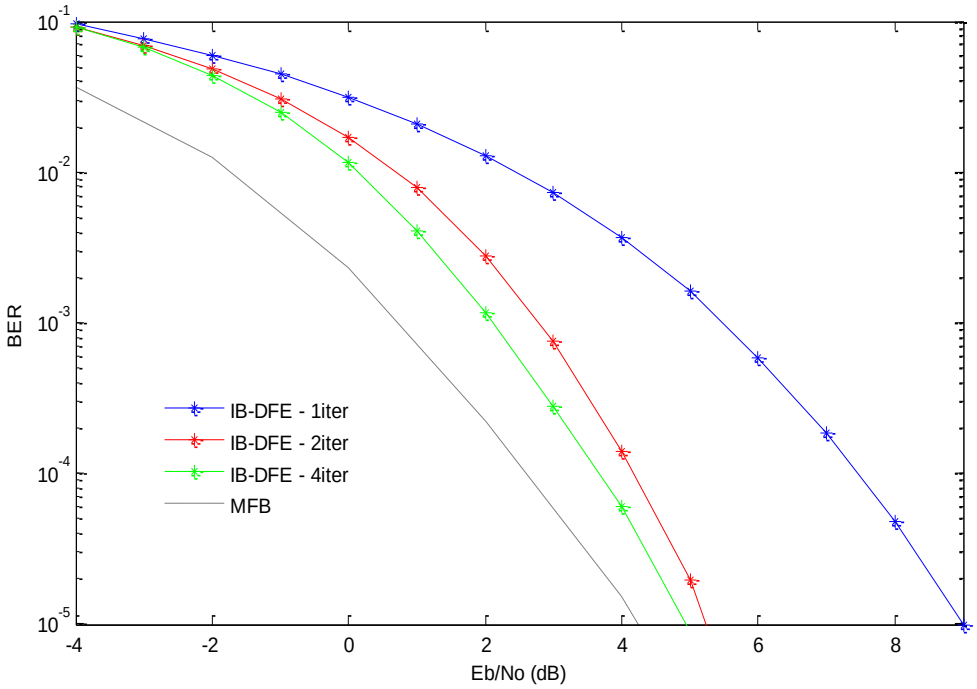

Figure 4.4 Performance evaluation at the central unit for scenario 1

- *Graphical results for scenario 2*

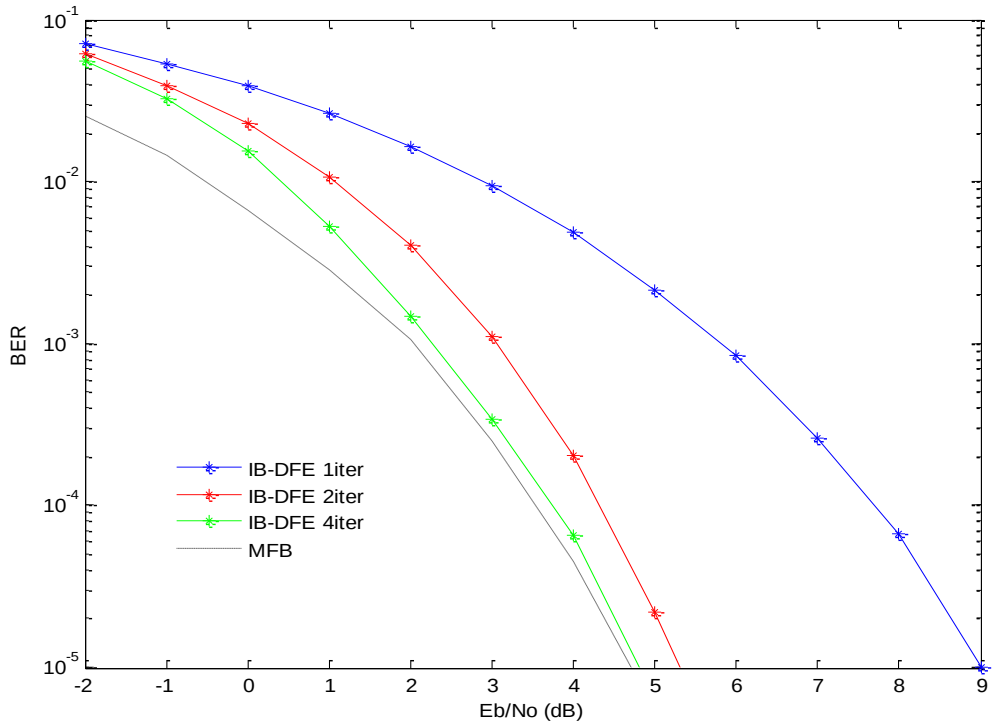

Figure 4.5 Performance evaluation at the macro-cell for scenario 2

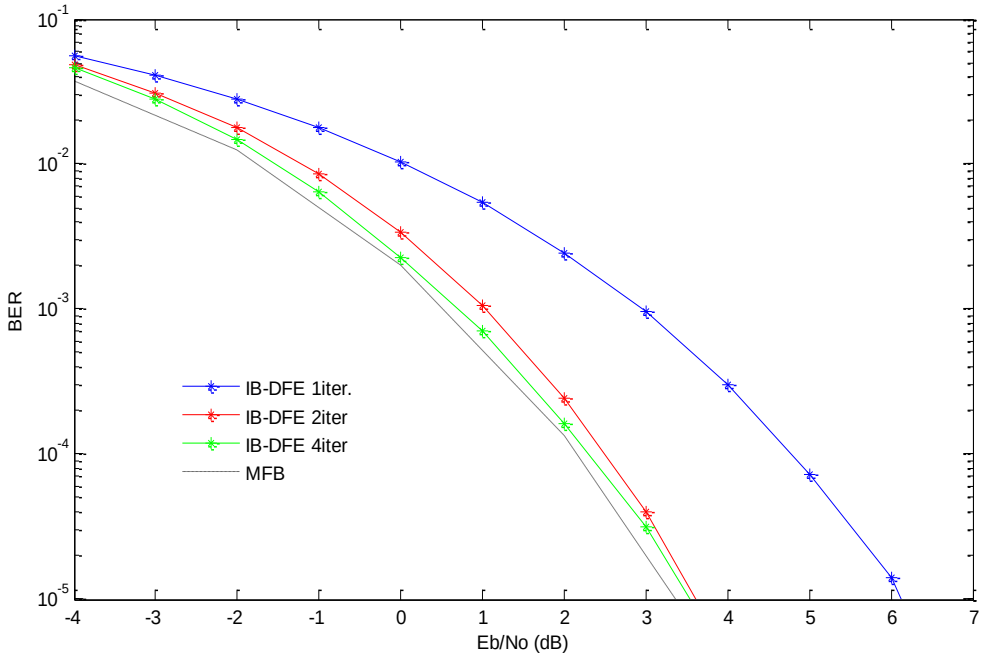

Figure 4.6 Performance evaluation at the central unit for scenario 2

Comparing now the results obtained at the CU for both scenarios (Figure 4.4 with Figure 4.6), we can see that for the second scenario, two iterations are enough to achieve the MFB performance. This is because, in the second scenario, the number of antennas at each terminal (APs and small-cell UTs) is larger (3 instead 2) and thus we have more DoF to efficiently separate the UTs data streams.

5. Conclusion and Future Work

5.1 Conclusion

The time when a mobile phone was used solely for conversation has long passed. More and more services and tools are used on a daily basis demanding a good quality of signal everywhere. YouTube, Facebook, and the many other applications that are of common use require larger and larger bandwidths. The diminished size of 4G tower coverage presents problems on cell edges, which can be reduced by the use of small cells cooperating with the macro cell, within its coverage area. These heterogeneous networks while a good idea, also have several problems. In order not to use precious bandwidth, small cells and macro cells use the same frequencies, greatly increasing interference. There are several techniques that help reduce this interference, of which interference alignment is one.

In this dissertation, we started by briefly presenting some of the reasons that promoted the evolution into the use of LTE and later LTE Advanced. The continuous need for more data throughput, and faster access times has led to the current generation of LTE. Having reached its limits in terms of good cell coverage, particularly in cell edges, new ideas are needed. That is where heterogeneous networks comes in. By using small cells to help areas of weaker coverage, a good quality of signal is assured.

In the second chapter, some multiple carrier and multiple access schemes were described. It was presented, in some detail, OFDM/A and SC-FDMA systems. OFDMA was deployed in the downlink of LTE systems, assuming an important role in wireless communications. Although OFDMA has high spectral efficiency and robustness against multipath fading, it has a high PAPR making it inefficient for the uplink as the power use on a mobile phone would be too high. That is where SC-FDMA come into play. Having the best properties of an OFDM system, but with a low PAPR, it is a good compromise as an uplink scheme. One easy way to increase data throughput without increasing the bandwidth is to take advantage of the use of more than one antenna. These extra antennas can be used to transmit or receive the same symbol, therefore improving the quality of reception, avoiding the need to resend data that had low quality, or to send more symbols, increasing the amount of data sent at a time.

In chapter 3, it was introduced the interference alignment techniques. These techniques allow to efficiently eliminate the inter-user interference, allowing us to achieve the maximum number of degree of freedom. Later in this chapter, iterative equalization was presented. It was seen that linear equalizers have low complexity, but suffer from noise enhancement and residual ISI. This allows the use of nonlinear equalizers that greatly outperform the linear ones. The focus here was on the iterative equalizer known as IB-DFE.

In chapter 4, a heterogeneous network with a set of small-cells overlaid over a macro-cell was considered. The terminals are SC-FDMA based devices. In the proposed scheme the small-cells precode their signals such that the interference generated at the macro-cell lies in a common subspace. To recover the macro-cell and small cells spatial streams, in the presence of both inter-system as well as inter-block and inter-carrier interferences, we designed IB-DFE based receivers. The matrices for these non-linear space-frequency equalizers were obtained by minimizing the overall mean square error of all data streams at each subcarrier.

The results have shown that the proposed receiver structures are robust to the inter-system interference and is able to efficient separate the spatial streams, while allowing a close-to-optimum space-diversity gain, with performance close to the MFB with only a few iterations of the equalizers.

5.2 Future Work

Concerning the future, the following changes can be applied to the current platform:

- In both scenarios, only 2 small cells were considered. It would be interesting to observe the results for more cells.
- The IB-DFE equalizer was built using the PIC approach. Even if the results would be somewhat similar, a SIC approach could be experimented on.
- Different IA algorithms can also be experimented.
- Evaluate the proposed system under imperfect channel information.

List of References

[1]. Harri Holma and Antti Toskala, "LTE for UMTS OFDMA and SC-FDMA Based Radio Access", John Wiley & Sons, Ltd. 2009.

[2]. "LTE Advanced: Heterogeneous Networks", Qualcomm Incorporated, January 2011.

[3]. Jeffrey G. Andrews, "Seven Ways that HetNets are a Cellular Paradigm Shift", *IEEE Communications Magazine*, p.136-144, March 2013.

[4]. 3GPP TR 36.839 v11.0.0, "Mobility Enhancements in Heterogeneous Networks (Release 11)", Sept. 2012.

[5]. M. Haenggi, "Stochastic Geometry for Wireless Networks", Cambridge University Press, 2012.

[6]. H. S. Dhillon et al., Modelling and Analysis of k-Tier Downlink Heterogeneous Cellular Networks", *IEEE JSAC*, Apr. 2012.

[7]. J. Hoadley and P. Maveddat, "Enabling Small Cell Deployment with HetNet," *IEEE Wireless Commun. Mag.*, vol 19, nº 2, pp 4-5, April 2012.

[8]. A. Goldsmith, S. Jafar, I. Maric, and S. Srinivasa, "Breaking Spectrum Gridlock with Cognitive Radios: An Information Theoretic Perspective," *Proceedings of the IEEE*, vol. 97, nº 5, pp. 894-914, May 2009.

[9]. V. Cadambe and S. Jafar, "Interference Alignment and Degrees of Freedom of the k-user Interference Channel," *IEEE Trans. Inf. Theory*, vol. 54, nº 8, pp. 3425-3441, Aug. 2008.

[10]. K. Gomadam, V. Cadambe and S. Jafar, "A Distributed Numerical Approach to Interference Alignment and Applications to Wireless Interference Networks", *IEEE Trans. Inf. Theory*, vol. 57, nº 6, pp. 3309-3322, June 2011.

[11]. S. W. Peters and R. W. Heath Jr., "Cooperative algorithms for MIMO interference channels", *IEEE Trans. Veh. Technol.*, vol. 60, nº 1, pp. 206-218, Jan. 2011.

[12]. W. Shin, W. Noh, K. Jang, and H.-H. Choi, "Hierarchical Interference Alignment for Downlink Heterogeneous Networks," *IEEE Trans. Wireless Commun.*, vol. 11, no. 12, pp. 4549–4559, December 2012.

[13]. S. Sharma, S. Chatzinotas, and B. Ottersten, "Interference Alignment for Spectral Coexistence of Heterogeneous Networks," *EURASIP Journal on Wireless Communications and Networking*, vol. 2013, no. 1, p. 46, Feb. 2013.

[14]. H. G. Myung, D. J. Goodman, *Single Carrier FDMA: A New Air Interface for Long Term Evolution*, John Wiley & Sons, 2008.

[15]. D. Falconer, S. Ariyavisitakul, A. Benyamin-Seeyar, B. Eidson. "Frequency Domain Equalization for Single-Carrier Broadband Wireless Systems." *IEEE Comm. Mag.*, vol. 40, no. 4, pp. 58-66, Apr. 2002.

[16]. N. Benvenuto, R. Dinis, D. Falconer, and S. Tomasin, "Single Carrier Modulation with Non Linear Frequency Domain Equalization: An Idea Whose Time Has Come - Again," *Proceedings of the IEEE*, vol. 98, no. 1, pp. 69-96, Jan. 2010.

[17]. OFDM-Based Broadband Wireless Networks – Design and Optimization, Hui Lui and Guoqing Li, John Wiley & Sons, Inc., 2005.

[18]. IEEE P902.16-2004 "Standard for local and metropolitan area networks Part 16: air interface for fixed broadband wireless access systems", European Telecommunications Standards Institute ETSI, January 1999.

[19]. M. Moeneclaey, M. Van Bladel and H.Sari, "Sensitivity of multiple-access techniques to narrow-band interference", IEEE Trans. On Commun., March 2001.

[20]. G.J. Pottie, "System design choices in personal communications", IEEE Personal Communication, vol. 2, nº 5, pp. 50-67, Oct. 1995.

[21]. Moray Rumney, "LTE and the Evolution to 4G Wireless", Agilent Technologies Publication, 2009

[22]. Ezio Biglieri, Robert Calderbank, Anthony Constantinides, Andrea Goldsmith, Arogyaswami Paulraj and H. Vincent Poor, "MIMO Wireless Communications", Cambridge University Press, 2007

[23]. Daniel Halperin, Wenjun Hu, Anmol Sheth and David Wetherall, " 802.11 with Multiple Antennas for Dummies", https://djw.cs.washington.edu/papers/mimo_for_dummies.pdf

[24]. G. J. Foschini and M. J. Gans, "On limits if wireless communications in a fading environment when using multiple antennas", Wireless Personal Communications, 6:311-335, 1998

[25]. 4G++: Advanced Performance Boosting Techniques in 4th Generation Wireless Systems, Work Package 4, Inter-Cell Interference Coordination

[26]. V.R. Cadambe and S.A. Jafar, "Interference Alignment and the Degrees of Freedom of Wireless X Networks", IEEE Transactions on Information Theory, vol. 55, pp. 3893-3908, 2009

[27]. H. Shen, B. Li and Y. Luo, "Precoding design using interference alignment for the network MIMO", IEEE 20th International Symposium on Personal Indoor and Mobile Radio Communications (PIMRC), pp. 2519-2523, 2009

[28]. Filipe Casal Ribeiro, "Multicell Cooperation for Future Wireless Systems", Dissertation presented in ISCTE-IUL, 2012

[29]. N. Benvenuto and S.Tomasin, "Block iterative dfe for single carrier modulation", Electronics Letters, vol. 38, no. 19, pp. 1144-1145, sep. 2002.

[30]. A.G. Dinis, R. and N. Esteves, "On broadband block transmission over strongly frequency-selective fading channels", Proc. Wireless, Jul. 2003

[31]. R. Dinis, P. Silva and T. Araújo, "Turbo Equalization with cancelation of Nonlinear Distortion for CP-Assisted and Zero-Padded MC-CDMA Schemes", IEEE Trans. On Commun. vol. 57, nº 8, pp. 2185-2189, Sp. 2009.

[32]. J. Luzio, R. Dinis and P. Montezuma, "SC-FDE for Offset Modulations: An Efficient Transmission Technique for Broadband Wireless Systems", IEEE Trans. On Commun. Vol 60, nº 7, pp. 1851-1861, Jul. 2012.